X

4 JRE

UNCLASSIFIED

MARTIN MARIETTA ENERGY SYSTEMS LIBRARIES
3 4456 0360753 1

CENTRAL RESEARCH LIBRARY
DOCUMENT COLLECTION

ORNL-1888
Engineering

FREE CONVECTION THEORY AND EXPERIMENT IN FLUIDS HAVING A VOLUME HEAT SOURCE

D. C. Hamilton
F. E. Lynch

CENTRAL RESEARCH LIBRARY
DOCUMENT COLLECTION

LIBRARY LOAN COPY

DO NOT TRANSFER TO ANOTHER PERSON

If you wish someone else to see this document, send in name with document and the library will arrange a loan.

OAK RIDGE NATIONAL LABORATORY
OPERATED BY
CARBIDE AND CARBON CHEMICALS COMPANY
A DIVISION OF UNION CARBIDE AND CARBON CORPORATION
UCC
POST OFFICE BOX P
OAK RIDGE, TENNESSEE

UNCLASSIFIED

ORNL-1888

Contract No. W-7405, eng 26

Reactor Experimental Engineering Division

FREE CONVECTION THEORY AND EXPERIMENT IN FLUIDS HAVING A VOLUME HEAT SOURCE

by

D. C. Hamilton and F. E. Lynch

Date Issued AUG 3 1955

OAK RIDGE NATIONAL LABORATORY
Operated by
CARBIDE AND CARBON CHEMICALS COMPANY
A Division of Union Carbide and Carbon Corporation
Post Office Box P
Oak Ridge, Tennessee

3 4456 0360753 1

ORNL 1888
Engineering

INTERNAL DISTRIBUTION

1. C. E. Center
2. Biology Library
3. Health Physics Library
5. Central Research Library
6. Reactor Experimental Engineering Library
7-11. Laboratory Records Department
12. Laboratory Records, ORNL R. C.
13. C. E. Larson
14. L. B. Emlet (K-25)
15. J. P. Murray (Y-12)
16. A. M. Weinberg
17. W. H. Jordan
18. S. J. Cromer
19. E. J. Murphy
20. E. H. Taylor
21. E. D. Shipley
22. C. E. Winters
23. J. A. Lane
24. F. C. VonderLage
25. J. A. Swartout
26. S. C. Lind
27. F. L. Culler
28. A. H. Snell
29. A. Hollaender
30. M. T. Kelley
31. C. P. Keim
32. R. S. Livingston
33. J. H. Frye, Jr.
34. G. H. Clewett
35. A. S. Householder
36. C. S. Harrill
37. D. S. Billington
38. R. N. Lyon
39. R. B. Briggs
40. A. S. Kitzes
41. O. Sisman
42. C. B. Graham
43. W. R. Gall
44. H. F. Poppendiek
45. S. E. Beall
46. J. P. Gill
47. P. R. Kasten
48. A. P. Fraas
49. P. N. Haubenreich
50. J. L. Wantland
51-110. D. C. Hamilton
111-120. F. E. Lynch
121. W. P. Walker
122. D. S. Toomb
123. S. J. Pias
124. G. L. Muller
125. R. H. Chapman
126. R. Van Winkle
127. R. E. Aven
128. H. W. Hoffman
129. N. F. Lansing
130. M. W. Rosenthal
131. W. D. Powers
132. H. C. Claiborne
133. L. G. Alexander
134. D. G. Thomas
135. M. A. Arnold
136. T. K. Carlsmith
137. W. K. Ergen
138. N. D. Greene
139. G. M. Adamson
140. E. S. Bettis
141. E. P. Blizard
142. A. D. Callihan
143. S. I. Cohen
144. G. A. Cristy
145. W. R. Grimes
146. W. D. Manly
147. L. A. Mann
148. E. R. Mann
149. W. B. McDonald
150. W. W. Parkinson
151. H. W. Savage
152. C. G. Larson
153. M. Tobias
154. L. E. McTaggart
155. L. F. Parsly
156. M. J. Skinner
157. R. B. Korsmeyer
158. H. C. Gray
159. R. I. Strough
160. A. Giangregorio
161. M. J. Skinner
162. ORNL Document Reference Library, Y-12 Branch
163. D. D. Cowen

EXTERNAL DISTRIBUTION

164. R. F. Bacher, California Institute of Technology
165. Division of Research and Medicine, AEC, ORO
166-454. Given distribution as shown in TID-4500 under Engineering category

DISTRIBUTION PAGE TO BE REMOVED IF REPORT IS GIVEN PUBLIC DISTRIBUTION

TABLE OF CONTENTS

	Page
SUMMARY	4
INTRODUCTION	5
NOMENCLATURE	9
BRIEF DESCRIPTION OF THE EXPERIMENT	13
The Apparatus	13
The Temperature Measurements	15
The Velocity Observations	16
THEORETICAL ANALYSIS FOR THE LAMINAR REGIME, MIDDLE REGION	17
The Velocity Solution	19
The Temperature Solution	20
An Approximate Analysis for $N_I < 10^4$	21
RESULTS AND DISCUSSION	23
The Velocity Structure	23
The Temperature Data	26
Development of the Parameter N_{III}	32
Middle Region Theory and Experiment	36
End Region Experimental Temperatures	38
CONCLUSIONS	42
REFERENCES	45
APPENDIX A: APPARATUS AND PROCEDURE	46
The Three-Parallel-Plates Apparatus	47
The Determination of $x_o(y,z)$	51
Instrumentation for Temperature Measurements	52
Procedure	56
APPENDIX B: TREATMENT OF THE DATA	59
Properties of the Electrolyte	59
Derivation of the Method for Computing $\theta_c^*(0,z)$	61
Derivation of the Method for Computing $\theta_c(0,z)$	67
The Data Analysis	68

SUMMARY

The free convection system investigated here consisted of two channels formed by three parallel and equally spaced vertical plates. The two channels were filled with a dilute electrolyte in which heat was generated uniformly by electrical resistance heating. The heat was transferred from the two free convection channels to the outer plates, then through the outer plates to the coolant channels in which the coolant was flowing vertically upward. The significant measurement was the temperature difference between the center wall and the outer wall at a given vertical level.

A Laminar Regime theoretical analysis was made based on the postulate that, in the Middle Region away from the ends, the velocity profile is fully established and the temperature is linear with the vertical coordinate.

Semi-quantitative visual observations of the paths of suspended droplets indicated that the free convection flow circuit exists as one long cell and that the velocity profile is fully established in the Middle Region and similar to that predicted by the theory. The onset of turbulence occurred at a Grashof modulus equal to 5×10^9, which is the same as for ordinary free convection.

For small values of the modulus, N_{III}, the vertical temperature gradient was uniform and the Middle Region Laminar Regime experimental temperature data were only 15 percent lower than the theory: For large values of N_{III} the vertical temperature gradient was not uniform and the temperature data were only 50 percent of the theoretical value. Above the critical value of Grashof modulus, the temperature data dropped sharply, due to turbulence, to about 66 percent of the laminar theory. In contrast to most convective heat transfer systems, the end region temperature differences near the top of the system were greater than those in the Middle Region.

INTRODUCTION

The effort represented by Reference 1 and the present work was directed toward an understanding of the heat transfer in a particular class of volume heat source free convection systems which may be described generally as follows:

1. The volume heat source is uniform.
2. The free convection system is a pipe or channel having a large ratio of length to diameter and oriented with the long axis vertical.
3. The bounding walls are cooled by forced convection with the coolant flowing vertically upward.

For each system geometry there are four separate problems to be investigated depending upon whether the flow is in the Laminar Regime or the Turbulent Regime and upon whether the region of interest is in the middle or near the ends of the system. The flow regime is determined by the value of the Grashof modulus relative to the critical value. The region classification is indicated in Figure 1. At a given height the minimum temperature in the free convection system is at the cooled wall while the maximum temperature is near the center of the pipe or channel. Near the top or bottom of the system, where the free convection dynamic and thermal boundary layers are initiated, the velocity and temperature profiles may vary rapidly with the vertical coordinate, z. At some distance from the ends of the system it is possible that the velocity and temperature profiles may become fully established and independent of z. The latter region is designated as the Middle Region and the former regions as the End Regions. At this point it should be emphasized that experimental proof of the existence of fully established velocity and temperature profiles in the Middle Region was not available when the present work was initiated. It had been

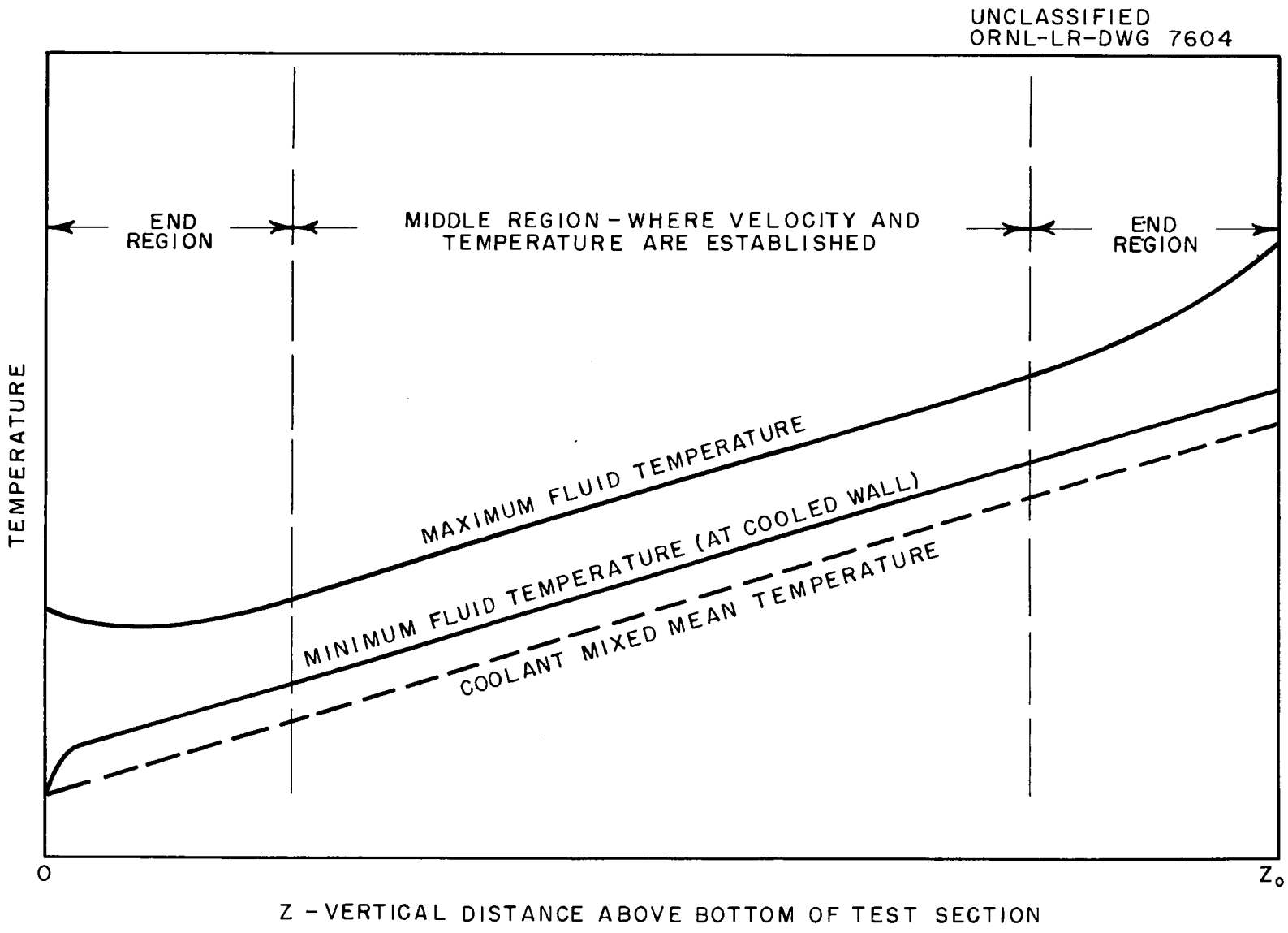

Fig. 1. Presumed Form of Temperature Distribution in Systems of Interest

suggested that, in the Laminar Regime, the free convection pattern might tend to exist as many laminar cells a few diameters long rather than as one long cell. If this were true, there could be no fully established Middle Region. One aim of the present investigation was to settle this question. For the purposes of the theoretical analysis the established profile Middle Region hypothesis was assumed and one of the principal objectives of the experimental program was the confirmation or denial of this hypothesis. The hypothesis can be written as two basic assumptions in the following manner:

1. $\frac{dw}{dz} = 0$; the vertical component of velocity is independent of z.
2. $\frac{dt}{dz} = A_c$; the vertical temperature gradient is uniform and equal to that of the coolant mixed mean temperature.

When these two assumptions are employed as postulates in a laminar flow system the differential equations become one dimensional and easily solved. These postulates were used in Reference 1 as the basis for Laminar Regime Middle Region analyses of the pipe and of the two-parallel-plates systems. A heat transfer experiment using either of these systems would require that fluid temperatures be measured; this would be a very difficult problem in a volume heat source free convection system. The three-parallel-plates system was chosen for the present investigation to avoid this difficulty.

The primary objective of the present work was to experimentally and theoretically investigate the heat transfer in the Laminar Regime Middle Region; however, some temperature measurements were also made in the Upper End Region because the significant temperature difference there was larger, and therefore more critical, than in the Middle Region. In most convective systems the reverse is true; that is, the temperature difference is minimum in the entrance region and approaches a maximum value in the established profile region.

Because it was assumed that most readers would not be interested in the details of the experiment, that information was placed in the appendix and only a brief description of the experiment is given as preparation for the discussion of the results. The theoretical analysis was left in the body of the report because the discussion of the postulates for the theory was believed to be a useful background for the understanding of the experimental results. In addition, it was from the theoretical analysis that the variables Φ, N_I and N_{II} were discovered which were used to analyze the experimental data.

NOMENCLATURE

$A = \frac{\partial t}{\partial z}$; vertical temperature gradient. (θL^{-1})*

In the theoretical analysis A was postulated to be uniform. In the experiment A actually was a function of both x and y, however only the values of A at or near z_a were used; thus, for these data A is reported as a function of X alone.

$A(0)$ = A at X = 0

$A(1)$ = A at X = 1

$A_a = \frac{1}{2}\left(A(0) + A(1)\right)$

A_c = A of the mixed mean coolant temperature.

c_p - Constant pressure specific heat. $(EM^{-1}\ \theta^{-1})$

$d = 2x_o$. (L)

E - electrical EMF. (V)

g - gravitational acceleration. (LT^{-2})

g_c - dimensional constant. $(LMF^{-1}\ T^{-2})$

k - thermal conductivity. $(ET^{-1}\ L^{-1}\ \theta^{-1})$

p - pressure. (FL^{-2})

P - power. (ET^{-1})

q - heat transfer rate. (ET^{-1})

q'' - heat transfer rate per unit area. $(ET^{-1}\ L^{-2})$

q''' - volume heat source term. $(ET^{-1}\ L^{-3})$

r - electrical resistivity of electrolyte. (RL)

---

*The dimensions of each symbol are given in terms of the energy (E), force (F), mass (M), length (L), time (T), temperature (θ), electrical resistance (R), electromotive force (V) system.

$t(X,z)$ - temperature. (θ)

$t_a = \frac{1}{2}\left(t(0,z_a) + t(1,z_a)\right)$; average temperature used to evaluate physical properties in N_I, N_{II}, N_{III}.

$t(m,z) = t(0,z) - \theta(0,z)F_1$

t_R - room air temperature.

v - volume occupied by the electrolyte in test section. (L^3)

w - z component of velocity. (LT^{-1})

$$\bar{w} = \frac{1}{x_i}\int_0^{x_i} w\,dx$$

x - coordinate. (L)

x_i - value of x at interface between the two free convection streams.

x_o - maximum value of x.

y - coordinate. (L)

$2y_o$ - width of apparatus test section. (L)

z - vertical coordinate. (L)
(z = 0 at bottom of test section)

z_o - maximum value of z. (effective length or height of test section)

$z_a = z_o/2$; average value of z.

z_u = 21.12 inches, location of upper center wall thermocouple.

z_m = 15.02 inches, location of middle center wall thermocouple.

z = 10.55 inches, location of lower center wall thermocouple.

NOTE: The following will explain the manner in which mean or integrated values are denoted:

if $u(x,y)$ varies over the ranges $-x_o < x < x_o$ and $-y_o < y < y_o$

then $u(x,m) = \frac{1}{2y_o}\int_{-y_o}^{y_o} u(x,y)dy$ and $u(m,m) = \frac{1}{2x_o 2y_o}\int_{-x_o}^{x_o}\int_{-y_o}^{y_o} u(x,y)dxdy$

Greek

$\alpha = \frac{k}{\rho c_p}$, molecular thermal diffusivity. $(L^2\ T^{-1})$

$\beta_v = \frac{1}{v}\frac{dv}{dt}$, volume temperature coefficient. (θ^{-1})

$\beta_r = \frac{1}{r}\frac{dr}{dt}$, electrical resistivity temperature coefficient. (θ^{-1})

$\beta_{rk} = \frac{1}{rk}\frac{d(rk)}{dt}$; (rk) temperature coefficient. (θ^{-1})

$\theta(X,z) = \left(t(X,z) - t(1,z)\right)$ - temperature excess above outer (cooled) wall temperature at the same value of z. (θ)

$\theta_c(0,z)$ - the value of $\theta(0,z)$ when all the heat is transferred by conduction in the x direction.

$\theta_c{*}(0,z) = \frac{q'''\ x_o^2}{2k}$; the value of $\theta_c(0,z)$ in a system where q''' and k are uniform with X.

$\lambda = \left(\frac{N_I}{64}\right)^{1/4}$

μ - dynamic viscosity. $(ML^{-1}\ T^{-1})$

$\nu = \frac{\mu}{\rho}$; kinematic viscosity. $(L^2\ T^{-1})$

ρ - mass density. (ML^{-3})

Dimensionless Functions

$N_{Nu} = \frac{q'' d}{k\ \theta(0)}$, Nusselt modulus; $N_{Nu} = \frac{4}{\Phi(0)}$ when $q'' = q''' d$ and $\theta_c(0) = \frac{q''' d^2}{8k}$

$N_{Pr} = \frac{\nu}{\alpha}$, Prandtl modulus

$N_{Gr} = \frac{z_o^3\ \beta g\ \theta(0,z_a)}{\nu^2} = \frac{1}{8}\ \Phi(0,z_a)\ N_{II} \left(\frac{z_o}{d}\right)^3$; Grashof modulus

$N_{Re} = \frac{\overline{w}\ 2x_1}{\nu}$, Reynolds modulus of free convection stream

$N_I = \frac{d^4 \beta g}{\alpha \nu} A$

$(N_I)_a$ - N_I computed with A_a

$(N_I)_c$ - N_I computed with A_c

$N_{II} = \frac{d^5\ \beta g\ q'''(m,z_a)}{k\ \nu^2}$

$N_{III} = \frac{N_{II}\ N_{Pr}}{1.4\ (N_I)_c} = \frac{q'''(m,z_a)\ d}{1.4\ k\ A_c}$

$\Phi(X,z) = \frac{\theta(X,z)}{\theta_c(0,z)}$, dimensionless temperature function

$\Phi(0,z) = \frac{\theta(0,z)}{\theta_c(0,z)}$, value of Φ at $X = 0$

$\left[\Phi(0,z)\right]_{min.}$, minimum value of $\Phi(0)$ observed in experiment

$\Phi_c(X,z)$ - the function Φ in a conduction system having no free convection

$\Phi^*(X) = \frac{\theta(X)}{\theta_c^*(0)}$

$W = \frac{wd}{\nu N_{II}}$, velocity function

$X = \frac{x}{x_o}$

BRIEF DESCRIPTION OF THE EXPERIMENT

The three-parallel-plates system to be experimentally and theoretically investigated is shown schematically in Figure 2. The free convection test section is formed by three parallel and equally spaced vertical flat plates. An additional parallel plate on each side forms a coolant channel. The experimental system was designed to approximate the following conditions:

Condition 1 - The volume heat source is uniform throughout the system and steady.

Condition 2 - The temperature and velocity are steady and two dimensional; that is, non-variant with the coordinate y, perpendicular to the paper.

Condition 3 - The ratio of height to channel width is large.

Condition 4 - The system is geometrically, dynamically, and thermodynamically symmetrical about the yz plane.

Condition 5 - The resistance to heat conduction in the walls, or plates, is small in the x direction and large in the y and z directions.

The Apparatus

The apparatus was formed by metal plates 8 in. wide by 36 in. high with a spacing, x_o, of 0.5 inches. The bottom and ends were made of plastic so that the only electrical path between the center wall and the two outer walls was through the fluid in the test section. A very dilute HCl solution was used as the electrolyte in the free convection test section. When an electrical potential difference was maintained between the center wall and the two

UNCLASSIFIED
ORNL-LR-DWG 7605

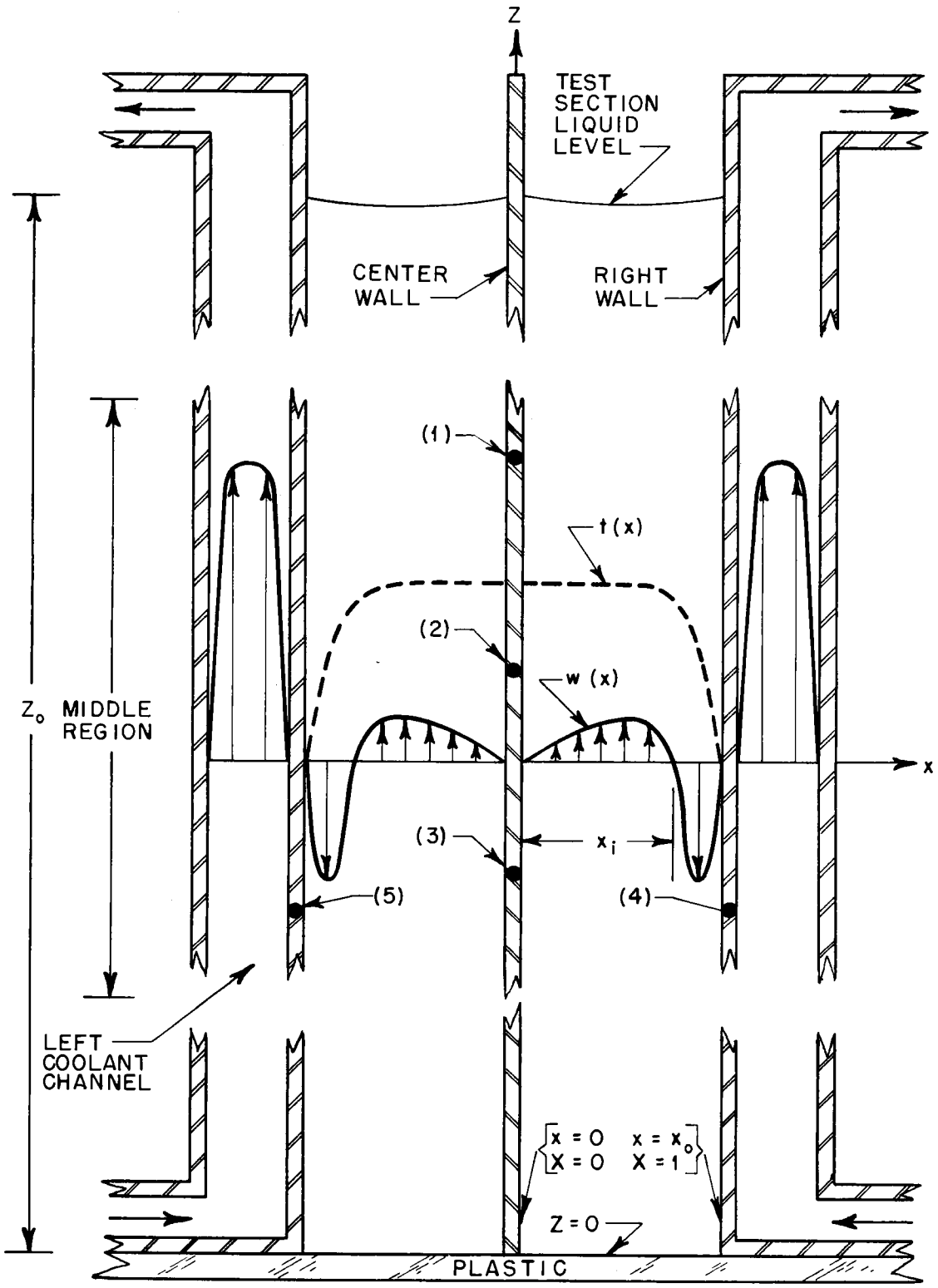

(1) UPPER CENTER WALL THERMOCOUPLE — FIXED AT $Z \cong 21$ inches
(2) MIDDLE CENTER WALL THERMOCOUPLE — FIXED AT $Z \cong 15$ inches
(3) LOWER CENTER WALL THERMOCOUPLE — FIXED AT $Z \cong 10.5$ inches
(4) RIGHT WALL THERMOCOUPLE } AJUSTABLE TO ANY POSITION FROM
(5) LEFT WALL THERMOCOUPLE } $Z = 0$ TO $Z = Z_o$

Fig. 2. Vertical Section Through XZ Plane of Three-Parallel-Plates System.

outer walls heat was generated within the volume of the fluid due to its electrical resistance. The volume heat source term, q''', was not uniform because the temperature coefficient of the electrolyte electrical resistivity was not zero. The average variation of the mean value of the volume heat source term, $q'''(m,z)$ was 5 percent for the Laminar Regime runs and 12 percent for the Transition Regime runs. A technique was derived for reducing the data to correspond to a system in which q''' is uniform.

The coolant flow rate and inlet temperature for each side and the total power could be set and accurately controlled over the following ranges: power, up to 15,000 Btu/hr: cooling water flow rate, up to 5,000 lbs per hour per side: cooling water inlet temperature, from 45°F to 120°F.

Temperature Measurements

In addition to the inlet and outlet coolant temperature thermocouples, three thermocouples were positioned in the center wall as shown in Figure 2 and a traversing thermocouple probe was provided in each outer wall which was adjustable to any vertical position. All temperature measurements were made in the xz plane. A junction box permitted the direct measurement of the temperature difference between any two junctions as well as the measurement of the temperature level of a particular junction above the ice point. The first 11 temperature runs were taken with the test section liquid level at 35 inches. In order to obtain temperature data in the End Region the level was lowered to about 22 inches for the remaining 17 runs. By this means temperatures could be measured to within about one inch of the effective top of the system.

Velocity Observations

In the development of the details of the design of the three-parallel-plate apparatus a two-plate apparatus was constructed which was identical with the three-plate apparatus used for the temperature measurements with three exceptions: First, the dimension, d, was 3/4 inches for the two-plate apparatus compared to one inch for the three-plate apparatus: Second, no wall temperature probe wells were provided: Third, there was no center wall. The qualitative or semi-quantitative velocity measurements were made with this two-plate apparatus using the technique developed in Reference 2. That technique involved the timing of the particle path for small oil droplets in the free convection system having the same density as the electrolyte and illuminated by a high intensity light beam. As was previously mentioned the heat transfer measurements were the primary objective of the experiment. Thus, the velocity observations made were limited to those believed to be necessary to the understanding of the temperature data. The purpose of the velocity experiment was to obtain the answer to the following five questions:

1. Does the free convection circuit exist as one long cell or as many short ones?

2. Does the velocity profile in the Middle Region become established and does it appear similar to the velocity profile given by the laminar theory?

3. What does the velocity structure look like in the End Region?

4. At what value of Grashof modulus does transition to turbulence occur?

5. Does the guard heater spacer design eliminate secondary flow (in the y direction) in the test section?

THEORETICAL ANALYSIS FOR THE LAMINAR REGIME, MIDDLE REGION

The conditions described in the previous section supply the first four of the postulates that define the Idealized System to be analyzed.

Postulate 1. q''' is uniform and steady.

Postulate 2. The temperature and velocity are independent of y and steady.

Postulate 3. The system is symmetrical about the yz plane.

Postulate 4. The resistance to heat conduction in the walls is zero in the x direction and infinite in the y and z directions.

Additional postulates required are:

Postulate 5. The free convection flow is in the Laminar Regime.

Postulate 6. All fluid properties except density are uniform.

Postulate 7. Density is uniform in the heat equation and is a linear function of temperature in the dynamic equation.

Finally, the two basic postulates discussed at length in the INTRODUCTION complete the definition of the system:

Postulate 8. There is one long convection cell so that in the Middle Region: $\frac{\partial w}{\partial z} = 0$

Postulate 9. The vertical temperature gradient, A, is uniform and equal to A_c.

As a consequence of Postulate 8 one can prove that the x components of velocity and pressure gradient vanish and that the vertical pressure gradient,

$\frac{\partial p}{\partial z}$, is uniform with x. The Navier-Stokes equations then reduce to:

$$\frac{d^2w(x)}{dx^2} = \frac{g_c}{\mu}\left(\frac{dp(z)}{dz} + \rho(x,z)\,\frac{g}{g_c}\right) \quad \ldots\ldots\ldots\ldots \quad (1)$$

As result of Postulate 9 it can be proven that the heat flux at the wall is uniform and therefore known; that is, each element of width, x_o, and height, dz, loses through its own bounding wall surface exactly the amount of heat generated within the element. Thus, no net heat loss occurs in the z direction for such an element. An additional consequence of Postulate 9 is that the use of the temperature function, θ, eliminates z as a variable; then the equations contain only one space variable, x.

The heat conduction equation is then simplified to:

$$\frac{d^2\theta(x)}{dx^2} = \frac{A}{\alpha}\,w(x) - \frac{q'''}{k} \quad \ldots\ldots\ldots\ldots\ldots\ldots\ldots \quad (2)$$

Or, in terms of dimensionless variables:

$$\frac{d^2\Phi(X)}{dX^2} = 2\,N_I\,W(X) - 2 \quad \ldots\ldots\ldots\ldots\ldots\ldots\ldots \quad (3)$$

Using a linear variation of density with temperature the density at any point in the system may be expressed as:

$$\rho(X,z) = \rho(1,z_a)\left[1 - \beta_v Az - \beta_v\theta(X)\right] \quad \ldots\ldots\ldots\ldots \quad (4)$$

Putting Equation (4) in Equation (1) get:

$$\frac{d^2w}{dx^2} + \frac{\rho(1,z_a)}{\mu}\,\beta_v\,g\theta(x) = \frac{g_c}{\mu}\,\frac{dp(z)}{dz} + \frac{g\rho(1,z_a)}{\mu}\left[1 - \beta_v Az\right] \quad \ldots \quad (5)$$

Since the left member of Equation (5) is a function of x alone and the right member is a function of z alone, each must be equal to a constant, say:

$$\rho(1,z_a)\left(\frac{\beta_v g q'''\,x_o^{\,2}}{2k\,\mu}\right) D$$

Setting the left member equal to this constant and making the variables dimensionless one obtains the velocity equation:

$$32 \frac{d^2W(X)}{dX^2} = D - \Phi(X) \quad \ldots\ldots\ldots\ldots\ldots\ldots\ldots \quad (6)$$

Velocity Solution

Differentiating Equation (6) twice and using Equation (3) to eliminate $\frac{d^2\Phi(X)}{dX^2}$, get:

$$\frac{d^4W(X)}{dX^4} + \frac{N_I}{16} W(X) = \frac{1}{16} \quad \ldots\ldots\ldots\ldots\ldots\ldots \quad (7)$$

The solution to Equation (7) is:

$$W(X) = \frac{1}{N_I} (1 + a \sin\lambda X \sinh\lambda X + b \cos \lambda X \cosh \lambda X + c \sin\lambda X \cosh \lambda X + d \cos \lambda X \sinh\lambda X) \ldots\ldots\ldots \quad (8)$$

$$\text{where } \lambda = \left(\frac{N_I}{64}\right)^{1/4}$$

The boundary conditions are:

(1) $W(0) = 0$

(2) The temperature is symmetrical about the z axis,

thus, $\frac{d\Phi(0)}{dX} = 0$

differentiating Equation (6), get $\frac{d\Phi(X)}{dX} = - 32 \frac{d^3W(X)}{dX^3}$

so $\frac{d^3W(0)}{dX^3} = 0$

(3) $W(1) = 0$

(4) Since there is no net flow

$$\int_0^1 W(X)\, dX = 0$$

Applying these boundary conditions to Equation (8) get:

$$\left.\begin{aligned} a &= -1-2\left[\frac{\sin^2\lambda + \sin\lambda\,\sinh\lambda - \lambda\,\sin\lambda\,\cosh\lambda - \lambda\,\cos\lambda\,\sinh\lambda}{\sinh^2\lambda - \sin^2\lambda}\right] \\ b &= -1 \\ c = d &= \left[\frac{(\cosh\lambda - \cos\lambda)(\sinh\lambda + \sin\lambda) - 2\lambda\,\sin\lambda\,\sinh\lambda}{\sinh^2\lambda - \sin^2\lambda}\right] \end{aligned}\right\} \quad \ldots \quad (9)$$

Thus:

$$N_I\,W(X) = 1 - \cos\lambda X\,\cosh\lambda X + a\,\sin\lambda X\,\sinh\lambda X + c(\sin\lambda X\,\cosh\lambda X + \cos\lambda X\,\sinh\lambda X) \ldots (10)$$

<u>Temperature Solution</u>

Since, by definition, $\Phi(1) = 0$ one gets, from Equation (6), the value of D and the temperature solution:

$$D = 32\,\frac{d^2W(1)}{dX^2}$$

$$\Phi(X) = 32\left(\frac{d^2W(1)}{dX^2} - \frac{d^2W(X)}{dX^2}\right) \quad \ldots\ldots\ldots\ldots\ldots\ldots \quad (11)$$

Differentiating Equation (10) and putting in Equation (11) get:

$$\Phi(0) = \frac{1}{\lambda^2}\left[\sin\lambda\,\sinh\lambda - a(1 - \cos\lambda\,\cosh\lambda) + c(\cos\lambda\,\sinh\lambda - \sin\lambda\,\cosh\lambda)\right] \ldots \quad (12)$$

$$\Phi(X) = \Phi(0) - \frac{1}{\lambda^2}\left[\sin\lambda X\,\sinh\lambda X - a(1-\cos\lambda X\,\cosh\lambda X) + c(\cos\lambda X\,\sinh\lambda X - \sin\lambda X\,\cosh\lambda X)\right] \quad \ldots\ldots\ldots \quad (13)$$

$$\lim_{\lambda\to\infty} \Phi(0) = \frac{1}{\lambda^2}(1 + 2\lambda) \quad \ldots\ldots\ldots\ldots\ldots\ldots\ldots\ldots \quad (14)$$

An Approximate Analysis for $N_I < 10^4$

For small N_I (or λ) values the following simplified analysis is accurate and much less laborious to solve numerically:

When Equation (10) is plotted for small N_I, X_i becomes equal to 0.5 and the velocity distribution in the hot and cold free convection streams corresponds to isothermal, laminar, forced flow in parallel plate channels. The velocity distribution may then be written as:

$$W(X) = \frac{24\ N_{Re}}{N_{II}}\ X(1-2X) \qquad \text{for } 0 \leq X \leq 0.5$$

$$W(X) = \frac{24\ N_{Re}}{N_{II}}\ (1-3X + 2X^2) \qquad \text{for } 0.5 \leq X \leq 1 \qquad \ldots\ldots\ldots \quad (15)$$

Setting the buoyant force equal to the friction force for the two streams, one obtains:

$$\int_0^{0.5} \Phi(X)dX - \int_{0.5}^{1} \Phi(X)dX = 12{,}288\ \frac{N_{Re}}{N_{II}} \qquad \ldots\ldots\ldots\ldots \quad (16)$$

Putting the velocity distribution from Equation (15) into Equation (3), integrating and applying the following boundary conditions one gets the temperature solution:

$$\text{b.c.} \ldots\ldots\ldots \frac{d\Phi(0)}{dX} = \Phi(1) = 0$$

$$\Phi(X) = 1-X^2 - \frac{N_{Re}\ N_I}{N_{II}}\ (1 - 8X^3 + 8X^4) \qquad \text{for } 0 \leq X \leq 0.5$$

$$\Phi(X) = 1-X^2 - \frac{8N_{Re}\ N_I}{N_{II}}\ (X - 3X^2 + 3X^3 - X^4) \qquad \text{for } 0.5 \leq X \leq 1 \qquad \ldots (17)$$

From Equations (16) and (17) get:

$$\Phi(0) = 1 - \frac{N_I}{12{,}288 + 1.4\ N_I} \qquad \ldots\ldots\ldots\ldots\ldots\ldots \quad (18)$$

and

$$N_{Re} = \frac{N_{II}}{1.4\ N_I + 1.23 \times 10^4} \quad \ldots\ldots\ldots\ldots\ldots\ldots\ldots \quad (19)$$

In summary, the dimensionless velocity and temperature function are dependent on only X and N_I as shown in Equations (10) and (13) while the free convection stream Reynolds modulus is dependent on both N_I and N_{II}, according to Equation (19). Equation (14) is accurate above N_I equal to 10^6 and Equations (17), (18), and (19) are valid for N_I less than 10^4. For $N_I = 0$ all solutions reduce to the "conduction only" solution, which is:

$$\begin{aligned} \Phi_c(0) &= 1 \\ \Phi_c(X) &= 1-X^2 \end{aligned} \quad \ldots\ldots\ldots\ldots\ldots\ldots\ldots\ldots \quad (20)$$

RESULTS AND DISCUSSION

The results of the velocity observations are discussed first to provide a background for the discussion of the thermal structure. Then a brief description is given of the manner in which the temperature measurements were converted to the dimensionless temperature modulus, $\Phi(0,z)$. Following this is given the development of the parameter, N_{III}, which permits prediction of the degree of uniformity of A. Finally, the heat transfer theory and experiment are given in dimensionless form. The comparison of the Middle Region Laminar Regime theory and experiment is the main objective and most important part of the investigation. The End Region experimental data are given, however, for whatever they may be worth.

The Velocity Structure

It is recalled that the velocity observations were made in a two-parallel-plate apparatus before the three-parallel-plate apparatus was constructed. The five questions concerning the velocity structure are discussed below in the same order in which they were posed in the section entitled BRIEF DESCRIPTION OF THE EXPERIMENT.

1. The free convection flow circuit existed as one long cell during all the observations made; even for Transition Regime flow conditions when the flow circuit would be momentarily broken by a large eddy the single cell pattern was resumed.

2. The velocity profile in the Middle Region did become established within the limit of accuracy of the present observations, and was similar to that given by the laminar theory in Reference 1. The profile observed in this region is shown in Figure 3.

3. In the upper End Region the velocity structure had the appearance of the free convection boundary layer growth near a cooled vertical plate immersed in a large pool. As shown in Figure 3

UNCLASSIFIED
ORNL-LR-DWG 7606

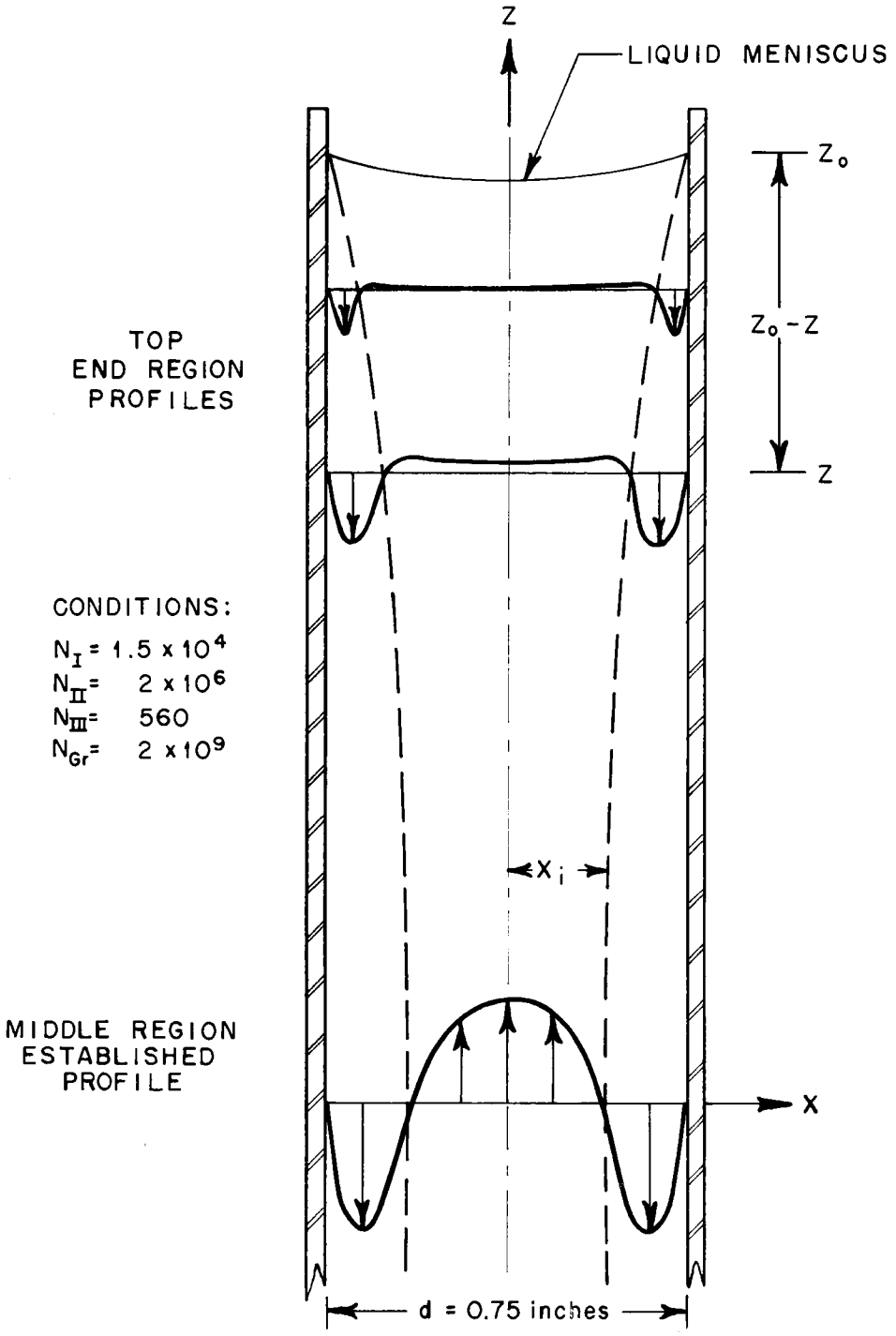

Fig. 3. Velocity Profiles Observed in A Two-Parallel-Plates System.

3. (Con't.)

the value of X_i was unity at the top of the system and decreased as $(z_o - z)$ increased. The velocity also increased with $(z_o - z)$. At some value of $(z_o - z)$, say $(z_o - z_e)$, the velocity profile seemed to become fully established; that is, the value of X_i and w became uniform with z. The length of this entrance region was observed to vary from 2d to 5d.

The lower End Region velocity structure was not investigated because screws in the plastic end plates obstructed the view.

4. The transition from laminar to mildly turbulent or transition type flow was observed to occur for a N_{Gr} equal to about 5×10^9. While keeping $N_I = 1.5 \times 10^4$, $N_{II} = 2 \times 10^6$, and $N_{III} = 560$, the apparatus was operated first for $N_{Gr} = 2 \times 10^9$ then for $N_{Gr} = 9 \times 10^9$ by filling the apparatus first to a level, $z_o = 20.3$ inches, then to a level, $z_o = 35.1$ inches.

A 16 f.p.s. movie film was taken of these two runs; in it the lower N_{Gr} run is clearly in the Laminar Regime and the higher N_{Gr} run is clearly in the Transition Regime. The Transition Regime run shows the sinuous, unsteady, snakelike motions in the center stream that are sometimes referred to as Schlicting waves. Eckert and Soehngen (Reference 3) have observed that, up to $N_{Gr} = 4 \times 10^8$, the free convection boundary layer must be laminar. Transition may occur at any N_{Gr} above this value, depending on many variables. The heat transfer data for ordinary free convection to vertical plates indicates a transition (by an abrupt change in slope) at $N_{Gr} = 4 \times 10^9$. The agreement between that value and the value for the present experiment suggests that the proximity of the two plates, thus two boundary layers, had little influence on the critical value of N_{Gr}.

5. No secondary flow was observed in the test section; secondary flow did exist, however, in the guard heater sections.

These observations in the two-parallel-plates system are submitted to be valid for the three-parallel-plates system. From these observations it is concluded that, for $N_{Gr} < 5 \times 10^9$ and in the Middle Region, the experimental system meets the hydrodynamic conditions described by the postulates of the ideal system theoretically analysed. The velocity structure according to the Laminar Regime Middle Region Theoretical Analysis for the three-parallel-plates system is given in Equation (10) as a function of N_I and N_{II}.

The Temperature Data

The dimensionless temperature distribution for the Laminar Regime, Middle Region, three-parallel-plates system theoretical analysis is shown in Figure 4 for several values of the parameter N_I. The value of $\Phi(X)$ at the center wall, $\Phi(0)$, is the only value that was determined experimentally. Thus, the values of $\Phi(0)$ from Figure 4 have been plotted versus N_I on subsequent graphs for comparison with the experimental data. In the Middle Region of a system in which q''' is uniform, $\Phi(0)$, is inversely proportional to the Nusselt modulus so $\Phi(0)$ is just a form of dimensionless heat transfer modulus that is more meaningful than N_{Nu} in a volume heat source system.

A summary of the important variables for each of the 28 runs is given in Table I. In many instances the number of significant figures given is greater than the accuracy of the number warrants; this was done to enable the reader to check the calculations or to compute the value of variables not listed. For example, the value of N_{Pr} at t_a may be read from Figure 14 in the appendix; then the Grashof modulus may be computed from tabulated values as follows:

$$N_{Gr} = N_{III}(N_I)_c \left(\frac{z_o}{d}\right)^3 \frac{\Phi(0,z_a)}{5.7\ N_{Pr}}$$

Similarly, A(0) may be computed by the equation:

$$A(0) = \frac{2\ A_a}{1+\frac{A(1)}{A(0)}}$$

The first 11 runs were taken with the apparatus filled to z_o equal to 35 inches. Since the uppermost center wall thermocouple was located at z_u = 21.1 inches no information concerning the value of $\Phi(0)$ in the End Region could be obtained. For the remaining 17 runs the apparatus was operated

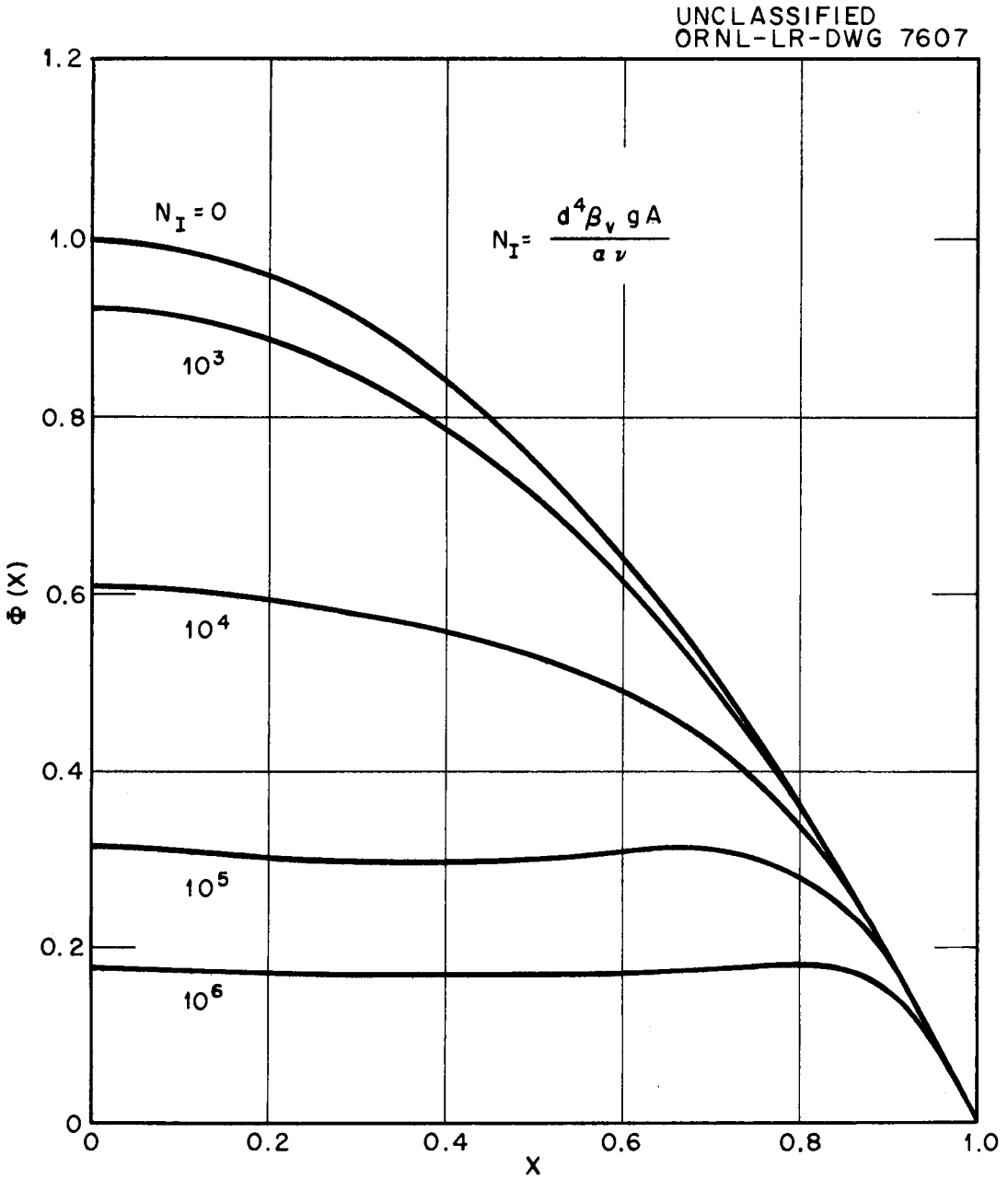

Fig. 4. Temperature in A Three-Parallel-Plates System According to the Laminar Theory (Equation 13)

TABLE IA

VALUES OF IMPORTANT VARIABLES FOR THREE-PARALLEL-PLATES SYSTEM HEAT TRANSFER EXPERIMENT

Run No.	z_o Inches	t_a °F	$q'''(z_a)$ B/hr ft^3	$\theta_c(0,z_a)$ °F	$A(1)/A(0)$	A_c °F/ft.	A_a °F/ft.	N_{III}	$(N_I)_a$	$(N_I)_c$
1	34.9	117.5	1.92×10^4	45.42	0.864	0.88	3.62	3550	1.38×10^5	3.35×10^4
2	35.1	144.0	1.06×10^5	247.00	0.845	4.60	15.72	3700	9.52×10^5	2.78×10^5
3*	34.8	109.5	3.39×10^3	8.08	0.456	0.13	1.00	4250	3.22×10^4	4.18×10^3
4	35.0	114.5	1.83×10^4	43.39	0.838	0.82	3.48	3650	1.25×10^5	2.94×10^4
5	35.0	128.0	1.79×10^4	42.15	0.976	7.65	8.81	380	4.09×10^5	3.55×10^5
6	34.8	112.0	3.13×10^3	7.42	0.902	1.25	1.75	410	5.96×10^4	4.26×10^4
7*	34.9	57.0	2.95×10^3	7.50	0.850	1.67	2.00	310	1.47×10^4	1.23×10^4
8*	35.0	50.5	2.64×10^3	6.81	0.450	0.19	0.94	2450	4.91×10^3	9.93×10^2
9*	35.0	49.2	7.52×10^2	1.94	0.300	0.10	0.20	1330	1.01×10^3	5.05×10^2
10*	34.7	63.5	2.73×10^3	6.88	1.024	2.83	2.92	170	2.53×10^4	2.45×10^4
11*	34.7	60.5	9.50×10^3	2.40	0.918	1.35	1.17	120	9.12×10^3	1.05×10^4
12*	24.0	65.0	2.68×10^3	6.74	0.949	3.25	3.24	140	3.01×10^4	3.02×10^4
13*	22.5	60.0	2.70×10^3	6.84	0.940	3.35	3.26	140	2.47×10^4	2.54×10^4
14*	22.3	47.6	8.88×10^2	2.31	0.572	0.21	0.38	750	1.74×10^3	9.63×10^2
15	22.5	118.0	3.10×10^3	7.32	0.710	0.90	1.80	560	6.90×10^4	3.45×10^4
16	22.5	121.0	6.54×10^3	15.42	0.810	2.46	3.71	430	1.52×10^5	1.01×10^5
17	22.2	126.0	1.38×10^4	32.50	0.630	2.50	5.10	900	2.29×10^5	1.12×10^5
18	22.1	129.7	2.09×10^4	49.15	0.692	4.26	7.43	800	3.52×10^5	2.02×10^5
19	22.4	130.7	5.13×10^4	120.30	0.753	2.71	14.20	3050	6.92×10^5	1.32×10^5
20*	22.7	78.5	1.56×10^3	3.83	0.407	0.09	0.76	2900	1.10×10^4	1.31×10^3
21*	22.7	57.3	9.57×10^2	2.44	1.038	1.40	1.34	120	9.29×10^3	9.70×10^3
22*	22.6	47.5	9.22×10^2	2.39	0.490	0.17	0.35	970	1.60×10^3	7.80×10^2
23*	22.6	49.7	9.39×10^2	2.43	0.725	0.34	0.60	490	3.01×10^3	1.70×10^3
24*	22.6	52.5	3.65×10^3	9.37	0.661	1.06	2.28	610	1.29×10^4	5.99×10^3
25	22.6	112.8	2.83×10^3	6.71	0.714	0.86	1.58	540	5.49×10^4	2.99×10^4
26	22.5	129.5	2.79×10^4	65.30	0.954	12.53	15.00	360	7.25×10^5	6.06×10^5
27	22.5	149.0	5.51×10^4	128.30	1.003	25.10	28.60	350	1.89×10^6	1.66×10^6
28	22.5	158.0	5.79×10^4	134.30	1.000	25.40	28.40	360	2.10×10^6	1.89×10^6

*Indicates Laminar Flow Runs; i.e. $N_{Gr} < 5 \times 10^9$

Note: In many cases more significant figures are given for a number than the accuracy warrants. This was done to permit the reader to check the calculations.

TABLE IB

VALUES OF IMPORTANT VARIABLES FOR THREE-PARALLEL-PLATES SYSTEM
HEAT TRANSFER EXPERIMENT

Run No.	$\theta(0,z_u)$ °F	$\theta(0,z_m)$ °F	$\theta(0,z_\ell)$ °F	$\Phi(0,z_u)$	$\Phi(0,z_m)$	$\Phi(0,z_\ell)$	$z_o - z_u$ Inches	$z_o - z_m$ Inches	$z_o - z_\ell$ Inches	$[\Phi(0,z)]_{min}$	$\Phi(0,z_o)$
1	7.60	7.14	7.35	0.167	0.158	0.164	13.8	19.9	24.3	0.158	
2	24.46	24.14	24.00	0.098	0.100	0.102	14.0	20.1	24.5	0.098	
3*	2.72	2.51	2.34	0.338	0.311	0.291	13.7	19.8	24.2	0.290	
4	8.22	7.15	7.46	0.189	0.166	0.174	13.9	20.0	24.4	0.165	
5	7.23	6.82	6.58	0.170	0.164	0.160	13.9	20.0	24.4	0.160	
6	2.10	1.92	1.92	0.282	0.260	0.261	13.7	19.8	24.2	0.258	
7*	3.65	3.40	3.16	0.486	0.457	0.427	13.8	19.9	24.3	0.400	
8*	4.58	4.29	3.99	0.676	0.635	0.593	13.9	20.0	24.4	0.570	
9*	1.46	1.40	1.27	0.756	0.720	0.657	13.9	20.0	24.4	0.600	
10*	2.80	2.77	2.87	0.406	0.406	0.424	13.6	19.7	24.1	0.400	
11*	1.53	1.42	1.34	0.638	0.594	0.565	13.6	19.7	24.1	0.530	
12*	3.22	2.56	2.51	0.470	0.379	0.375	2.9	9.0	13.4	0.370	0.60
13*	3.47	2.91	2.82	0.498	0.422	0.414	1.4	7.5	12.0	0.410	0.52
14*	2.23	1.68	1.58	0.970	0.730	0.687	1.6	7.7	12.2	0.680	1.00
15	2.33	1.65	1.48	0.316	0.225	0.203	1.4	7.5	12.0	0.200	0.36
16	4.18	3.32	2.94	0.267	0.214	0.191	1.4	7.5	12.0	0.170	0.28
17	9.42	7.35	6.37	0.283	0.225	0.197	1.7	7.8	12.3	0.165	0.30
18	12.84	9.90	8.79	0.252	0.200	0.180	1.8	7.9	12.4	0.170	0.28
19	25.08	18.01	15.37	0.197	0.147	0.128	1.5	7.6	12.1	0.115	0.22
20*	2.22	1.58	1.34	0.577	0.414	0.351	1.6	7.7	12.2	0.300	0.65
21*	1.56	1.23	1.23	0.635	0.505	0.506	1.6	7.7	12.2	0.500	0.74
22*	2.36	1.80	1.69	0.988	0.756	0.710	1.5	7.6	12.1	0.710	1.00
23*	2.13	1.74	1.67	0.876	0.718	0.689	1.5	7.6	12.1	0.680	0.95
24*	5.92	8.90	4.47	0.623	0.522	0.480	1.5	7.6	12.1	0.440	0.66
25	2.18	1.49	1.34	0.322	0.222	0.200	1.5	7.6	12.1	0.195	0.38
26	12.90	10.40	10.09	0.186	0.156	0.156	1.4	7.5	12.0	0.155	0.20
27	19.30	15.02	14.47	0.137	0.113	0.114	1.4	7.5	12.0	0.111	0.14
28	19.32	14.32	14.09	0.132	0.104	0.106	1.4	7.5	12.0	0.101	0.14

*Indicates Laminar Flow Runs; i.e. $N_{Gr} < 5 \times 10^9$

Note: In many cases more significant figures are given for a number than the accuracy warrants. This was done to permit the reader to check the calculations.

using values of z_o between 22 and 24 inches; this placed the top of the system near enough to the upper center wall thermocouple so that the $\Phi(0,z)$ data could be extrapolated to z_o. There was some question at this time as to whether or not the 22 inch high system was long enough to give $[\Phi(0,z)]_{min.}$ values in the Middle Region that would still be characteristic of a "long" system. The excellent agreement of Runs 12 and 13 with Run 10 gave the authors confidence that the 22 inch system was long enough; thus, all subsequent runs were made using the lower level.

The conditions of the runs were chosen to give data over the widest range possible with the present apparatus. As a result of this attitude 14 runs were in the Laminar Regime and 14 runs were in the Transition Regime. The runs in the Laminar Regime are indicated in Table I.

The temperature data for Run No. 5 are shown in Figure 5. The left wall temperature was lower than the right wall temperature for all of the runs and the depression was greater for $19 < z < 30$. After the experiments were concluded the apparatus was disassembled; the left wall thermocouple probe well tubing was found to be unsoldered. In the 19 inch to 30 inch region that tubing was not even touching the wall so it was probably reading a temperature closer to the coolant mixed mean temperature than to the wall temperature. Inspection of the right wall well tubing proved it to be in good condition. On the basis of the above information the left wall temperature was not used and the data were analysed using the right wall temperatures.

In addition to the value of $\theta(0,z)$ at z_ℓ, z_m and z_u, which were measured directly, the values for A(0) and A(1) were desired. The t(1,z) data for all the runs were linear with z as shown in Figure 5. A(1) was determined graphically from a straight line drawn through the points. In many instances, particularly

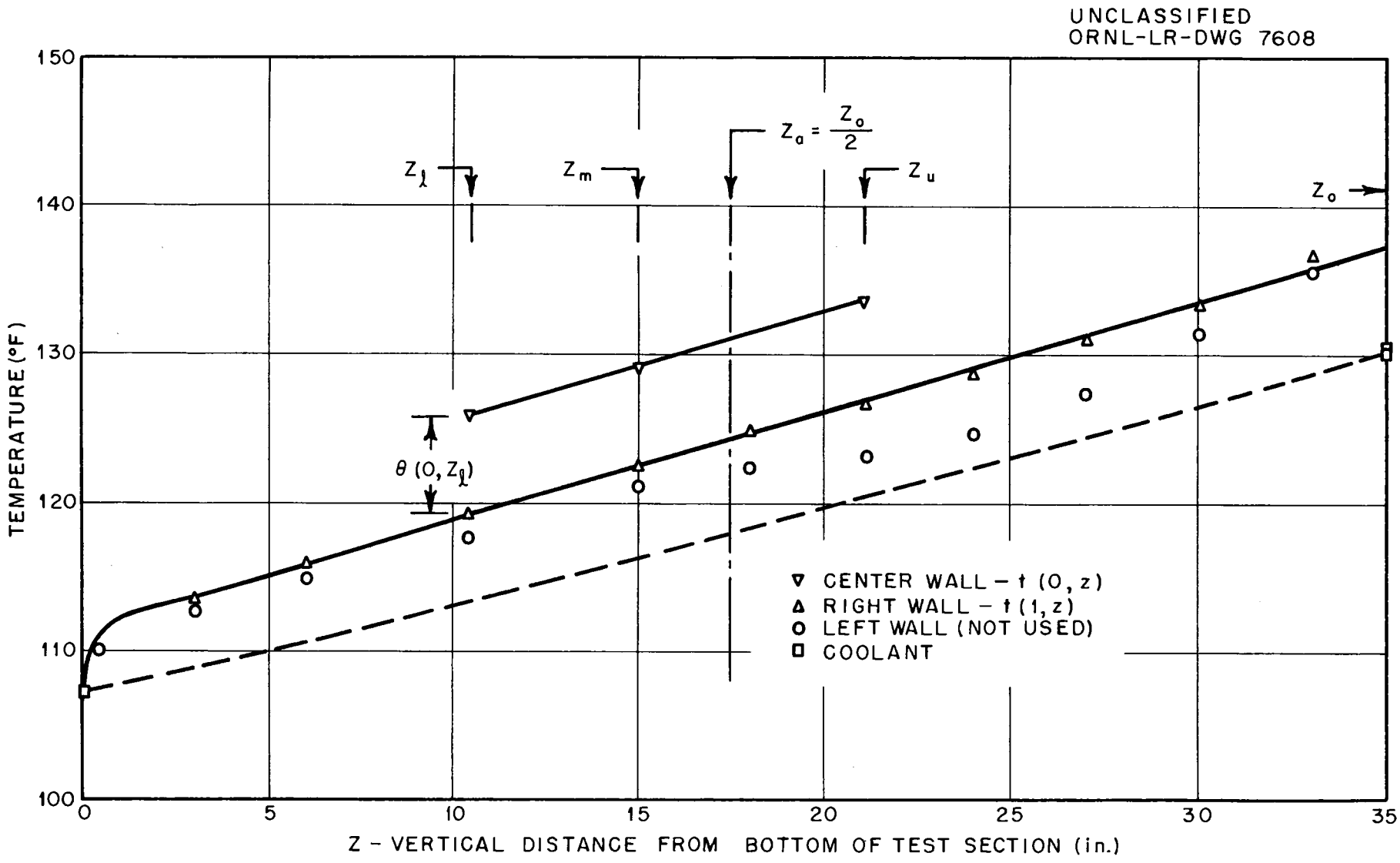

Fig. 5. Sample Temperature Data (Run No. 5)

the $z_o \cong 22$ runs, the three center wall temperatures were not colinear. Since it was the value of A(0) in the Middle Region that was desired, that value was obtained from direct measurements of $\left[t(0,z_m) - t(0,z_\ell)\right]$ and the known value of $(z_m - z_\ell)$.

The $\Phi(0,z)$ data for five typical runs are shown in Figure 6. For the data typified by Runs 19, 21, and 25 the extrapolation to obtain $\Phi(0,z_o)$ is not difficult. Similarly, the minimum value for each curve, $\left[\Phi(0,z)\right]_{min.}$, is easily determined for the data typified by Runs 6, 21, and 25. The minimum value was less obvious for Runs 7 and 19 and their associated runs. The data typified by Run 7 suggest that the temperature profile did not become established for those runs.

Development of the Parameter N_{III}

It is recalled that one important objective of the experiment was to test the validity of two basic assumptions concerning the Middle Region; these were:

1. $\frac{dw}{dz} = 0$; the vertical component of velocity is independent of z.

2. $\frac{dt}{dz} = A_c$; the vertical temperature gradient is uniform and equal to that of the coolant mixed mean temperature.

In the discussion of the velocity observations it was concluded that the first assumption was valid. In the discussion below it will be concluded that the second assumption is usually valid when the variable N_{III} is less than 400 and usually not valid for N_{III} greater than 1300.

The conclusions about A must be reached using the limited data available; specifically, measurements were made of A(0), A(1), and A_c. Convincing proof that A <u>is</u> uniform would require measurements within the free convecting fluid

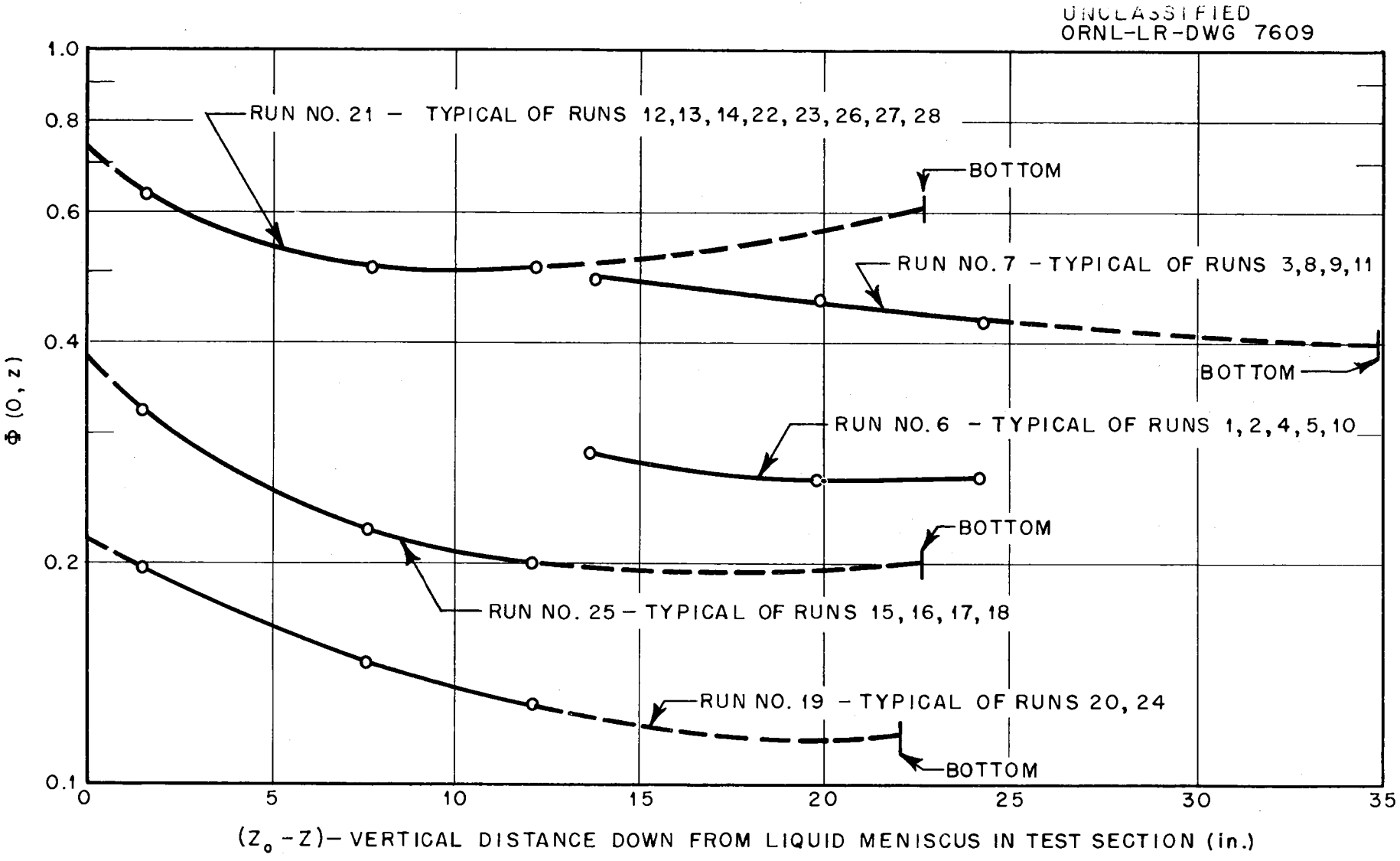

Fig. 6. Vertical Distribution of Temperature Function, $\Phi(O, z)$ (For Five Typical Experimental Runs)

itself; however, if A(1) and A(0) are not equal, it can be concluded that A is not uniform. The uniformity of A for the experimental system may be expressed as the condition where $A(0)/A(1) \cong 1$. Now, A may be fairly uniform (say $A(0)/A(1) > 0.8$) yet differ from A_c by a factor of ten.

The gradient in the coolant, A_c, is easily predicted from the power and coolant flow rates but A(0) and A(1) cannot be predicted. Thus, a useful correlation must be based on $(N_I)_c$, if $(N_I)_c$ and $(N_I)_a$ are different. Since A_c is dependent only on the power and the coolant flow rate, each of which may be independently controlled, A_c itself is therefore an independent variable in a system; however, A in the free convection system is not an independent variable, but is determined by the free convection system. For the purposes of this discussion let the free convection flow be visualized as two parallel counterflow streams; i.e. the ideal system model used in the approximate analysis. The heat generated in the center, warmer, and upward flowing stream is eliminated by two methods; part of the heat is transferred by pure conduction in the x direction to the outer, cooler, and downward flowing stream; the rest of the heat is dissipated from the center stream by convection. Precisely the same amount of heat is convected into the outer stream (because the product Aw is negative in that stream). This may be stated mathematically as follows:

$$(N_{Re}\, N_{Pr})\, A_a = Q \qquad (21)$$

where Q is proportional to the ratio of the amount of heat transported from the center stream to the outer stream by convection to the total heat generated in both streams. For the moment let the discussion be confined to a system in which the power, physical properties, and dimensions are held constant and only the coolant flow rate will be varied; under these conditions Q in Equation (21)

will be constant. Recall that, from the analysis of a system in which A is uniform, the free convection Reynolds modulus was given by:

$$N_{Re} = \frac{N_{II}}{1.4\ N_I + 1.23 \times 10^4} \quad \ldots\ldots\ldots\ldots\ldots \quad (19)$$

For $N_{II} > 10^6$ the constant in Equation (19) is negligible and the following can be written:

$$N_{Re}\ N_{Pr} = \left(\frac{N_{II}\ N_{Pr}}{1.4\ N_I}\right) \quad \ldots\ldots\ldots\ldots\ldots\ldots\ldots \quad (19a)$$

Let N_{III} be defined as the value of $N_{Re}\ N_{Pr}$ for a system in which A is uniform and equal to A_c; i.e.

$$N_{III} \equiv \frac{N_{II}\ N_{Pr}}{1.4\ (N_I)_c} \quad \ldots\ldots\ldots\ldots\ldots\ldots\ldots\ldots \quad (19b)$$

Let it be assumed that the experiment is begun by choosing values of power and coolant flow rate so that A is uniform and equal to A_c. Now Equation (21) demands that Q units of heat must be convected out of the inner stream. As A_c, and therefore $(N_I)_c$, is decreased the value of $N_{Re}\ N_{Pr}$ must be increased to the new value of N_{III} in order to maintain the system with a uniform A. The $N_{Re}\ N_{Pr}$ is determined by the temperature profile and the friction factor. One might expect that, if A_c, or $(N_I)_c$, are lowered sufficiently, a point would be reached when the buoyant forces in the system could not produce a value of $N_{Re}\ N_{Pr}$ as great as that called for by N_{III}. That is: $N_{Re}\ N_{Pr} < N_{III}$. In order to satisfy Equation (21) the value of A in the center stream must be greater than A_c, or:

$$(N_{Re}\ N_{Pr})\ A_a = (N_{III})\ A_c \quad \ldots\ldots\ldots\ldots\ldots\ldots \quad (22)$$

Then A is no longer uniform. It is proposed that, for N_{III} less than some critical value, $A_a \cong A_c$ and $N_{III} \cong N_{Re}\ N_{Pr}$, and above this value $\frac{A_c}{A_a} = \frac{N_{Re}\ N_{Pr}}{N_{III}} < 1$.

This, then, is the reasoning used to support the use of N_{III} as a variable for predicting the non-uniformity of A in the present system. The critical value of N_{III} must be determined from experiment.

Middle Region Theory and Experiment

The 28 runs have been grouped in Table II according to the value of N_{III}; the influence of that parameter on $A(1)/A(0)$ and A_c/A_a is apparent.

TABLE II

INFLUENCE OF N_{III} ON A

Group No.	No. of Runs	N_{III} Range	$[A(1)/A(0)]_{ave.}$	$[A_c/A_a]_{ave.}$
I	10	$N_{III} < 400$	0.96	0.95
II	8	$1300 < N_{III}$	0.61	0.24
III	10	$400 < N_{III} < 1300$	0.69	0.56

The influence of N_{III} on $[\Phi(0,z)]_{min.}$ is shown in Figure 7. Realizing that A_c, thus $(N_I)_c$, are the only values one can predict in designing a system, it is apparent that $[\Phi(0,z)]_{min.}$ for Group II would be approximately half that which one would calculate. From Figure 7 and Table II one concludes that for $N_{III} > 1300$, A is not uniform and not equal to A_c; for $N_{III} < 400$, A is uniform and is approximately equal to A_c. In addition, the Group I points agree more or less with the laminar theory (in the laminar regime) while the Group II points are about 50 percent low.

In this experiment a concerted effort was made to cover as wide as possible a range of all the variables. To obtain an $N_{III} > 1300$ one must use an excessively high, possibly uneconomically high, coolant flow rate for a given power. It seems quite possible, then, that the $N_{III} > 1300$ range would not be chosen in a design.

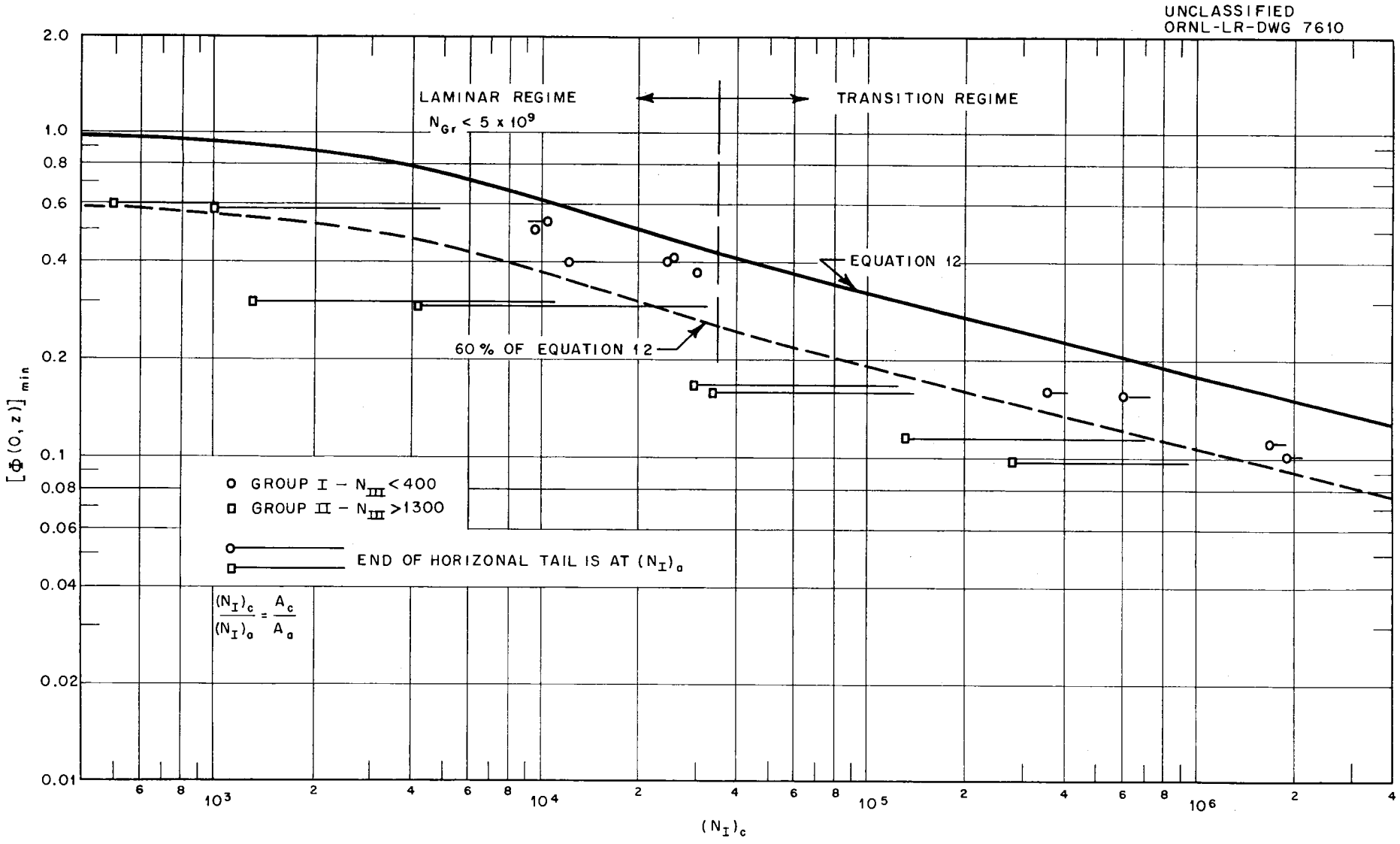

Fig. 7. Influence of N_{III} on Minimum $\Phi(0,z)$

The Groups I and III data, that is $N_{III} < 1300$, are shown in Figure 8 using $(N_I)_a$ as abscissa and the Laminar Regime Middle Region Theory, Equation (12), as a reference. The theory is, of course, not applicable in the Transition Regime above the critical value of N_{Gr}. In the present experiment $(N_{Gr})_{cr.}$ occurred at a value of $(N_I)_a$ of about 3×10^4. In a different system this might occur at higher or lower values of $(N_I)_a$.

The Groups I and III Laminar Regime data fall about a line that is 80 percent of the theory and with a scatter of $\pm$ 8 percent. Recall that the theory was based on the postulate that A is uniform. If $A(1)/A(0) > 0.9$ is used as the criterion for the uniformity of A it is seen that those points are only 15 percent lower than the theory; i.e. a line that is 85 percent of Equation (12) . The measured value of $\theta(0,z)$ could have been too small by no greater than 5 percent due to conduction in the walls in the y direction. Secondary free convection flow, in the y direction, could also cause $\theta(0,z)$ to be low; the velocity observations indicated that no such flow occurred. Thus, the remaining 10 percent cannot be specifically accounted for.

The Transition Regime $[\Phi(0,z)]_{min.}$ data lies in a relatively narrow band and, as would be expected, is lower than the Laminar Regime data.

End Region Experimental Temperatures

The maximum value, $\Phi(0,z_o)$, of the function is plotted in Figure 9 versus $(N_I)_a$ for all 17 runs in which z_o was about 22 inches. In any convection system the walls form a definite part of the entire heat transfer system. The resistance to heat conduction along the walls may assume any value from zero to infinity and the magnitude of this resistance may greatly influence the thermal structure in the convection system in some cases. This is especially true in free convection where the convective conductances are relatively small. In the

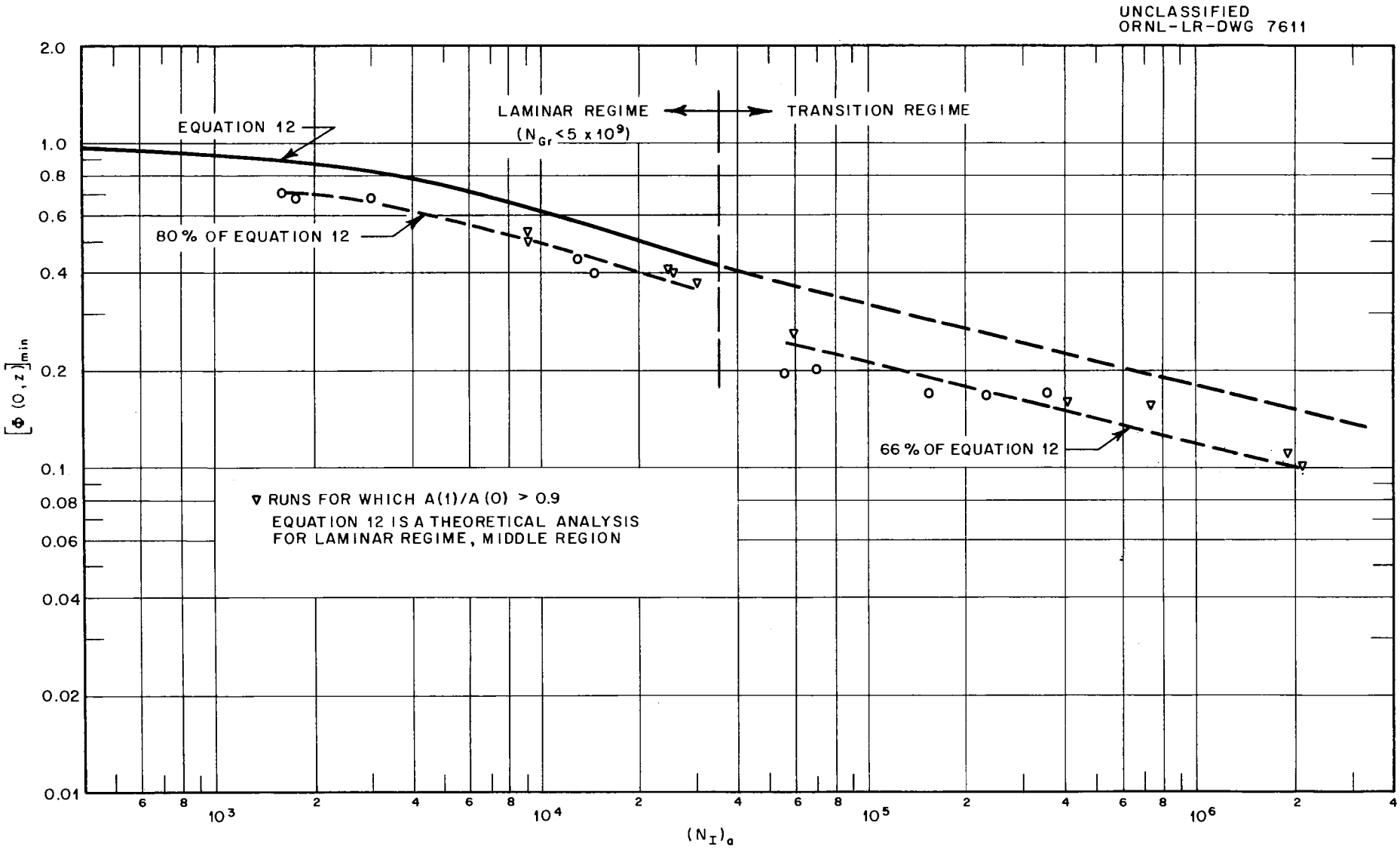

Fig. 8. Variation of Minimum $\Phi(0, z)$ with $(N_I)_a$ (For $N_{III} < 1300$)

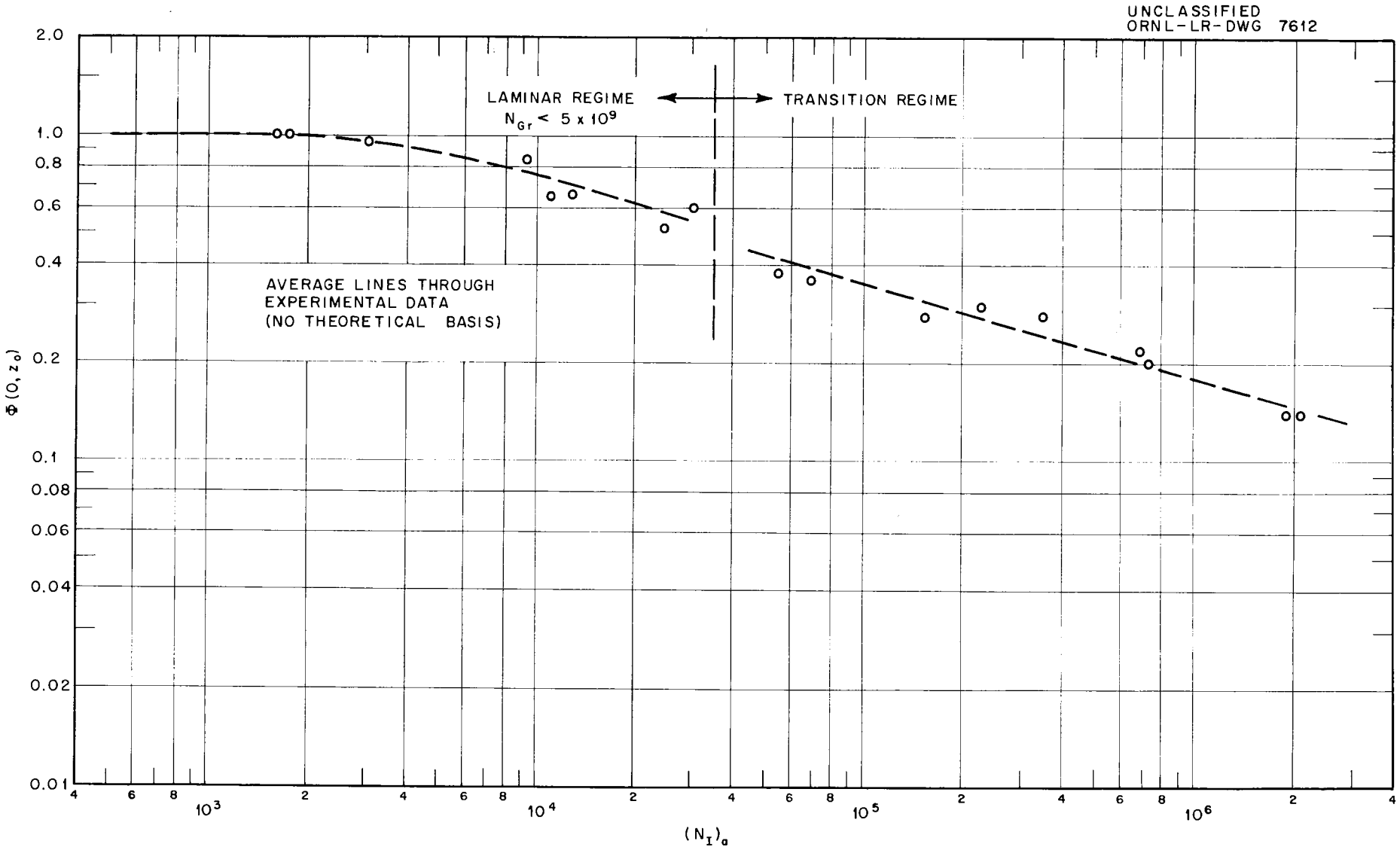

Fig. 9. Variation of Maximum $\Phi(0,z)$ with $(N_I)_a$

present system the wall resistances in the z direction are relatively small; this has virtually no influence on the system in the Middle Region where the temperature is everywhere linear with z and where the wall heat flux is uniform. In the End Region the situation is very different. The temperature in the free convection stream is definitely not linear with z, the wall flux is certainly not uniform with z, and the free convection system stops at the liquid meniscus whereas the wall continues for 14 inches above the meniscus. The present apparatus was designed to optimize the construction of an apparatus instrumented for Middle Region measurements. These Middle Region measurements are believed to be relatively precise and of general application. The End Region data are specific and may apply only to the present apparatus. The proper investigation of the End Region would require a program many times greater in scope and length than the present investigation. The present data are submitted to prove only that the End Region data are higher than the Middle Region data.

CONCLUSIONS

The following conclusions concerning the velocity structure may be made from the observations of droplet paths in the two-parallel-plates apparatus:

(1) The free convection flow circuit in such systems exists as one cell or loop of length equal to the height of the system.

(2) In the upper End Region the velocity structure has the appearance of the free convection boundary layer near the top of a cooled vertical plate immersed in a fluid.

(3) The transition from laminar to turbulent boundary layer occurs at approximately the same value of Grashof modulus as in a single vertical plate system: This was about 5×10^9.

(4) The free convection velocity profile appears fully established in the Middle Region and is similar to that given by the Laminar Regime Middle Region theoretical analysis.

It is emphasized that the velocity observations were not numerous and not precise. A much more extensive experimental program would be required to illuminate any subtle deviations in the flow from that described above.

A Laminar Regime Middle Region theoretical analysis was made which described the temperature and velocity structure in a three-parallel-plates system. The principal postulates in this analysis were:

(a) The volume heat source term is uniform.

(b) The velocity profile is fully established.

(c) The vertical temperature gradient, A, is uniform.

There were 28 runs made in the experimental counterpart of the above system in which heat transfer, or temperature data, were taken: Half of these runs were in the Laminar Regime and half were in the Turbulent Regime. The total vertical variation in the volume heat source term averaged 5 percent for the Laminar Regime runs and 12 percent for the Turbulent Regime runs; this is

considered to satisfy the requirement in (a) above. It was previously stated in conclusion (2) above that postulate (b) was satisfied. The Middle Region data were of greatest interest; however, End Region temperature data were also taken for 17 of the 28 runs.

The theory and experiment pertaining to the temperature in a three-parallel-plates system suggests the following conclusions, all but the last of which pertain to the Middle Region.

(5) The vertical temperature gradient, A, is not uniform for all conditions and may differ from A_c, the value in the coolant, by as much as a factor of 10. For the present experiments, at least, the dimensionless modulus, N_{III}, appears to be a good indicator of whether or not A will be uniform and equal to A_c in the system.

(6) For the 10 runs having $N_{III} < 400$, called Group I, the average values of $A(1)/A(0)$ and A_c/A_a were 0.96 and 0.95, respectively: For the 8 runs having $N_{III} > 1300$, called Group II, the average values of $A(1)/A(0)$ and A_c/A_a were 0.61 and 0.24, respectively. It is concluded from this that A is apparently uniform and equal to A_c for $N_{III} < 400$ and definitely not uniform for $N_{III} > 1300$. Fortunately, it seems doubtful that the combination of coolant flow rate and power required to satisfy $N_{III} > 1300$ would be of practical interest.

(7) The Laminar Regime dimensionless temperature modulus for the five experimental runs meeting the requirements of uniformity of A were approximately 15 percent lower than the values predicted by the Laminar Regime, Middle Region theory. All Laminar Regime runs having $N_{III} < 1300$ fell about a line 20 percent lower than the theory with a scatter of ± 8 percent. It is concluded from this that theory and experiment are in satisfactory agreement when the experimental system satisfies the postulates of the ideal system; these requirements are satisfied, in general, when N_{III} is small. As N_{III} is successively increased, while maintaining the same value of $(N_I)_c$, the values of $A(1)/A(0)$, A_c/A_a and $[\Phi(0,z)]_{min.}$ appear to be successively decreased.

(8) Above the critical value of Grashof modulus the temperature data dropped abruptly, due to the turbulence, to an average value of about 34 percent lower than the laminar

(8) Continued

theory. The influence of N_{III} was the same as for the Laminar Regime data.

(9) The Upper End Region temperature data indicated that $\Phi(0,z)$ is always greater in that region than in the Middle Region. This is equivalent to the statement that the heat transfer coefficient is lower in the entrance or end region than in the established or middle region; the opposite is true in most other convection heat transfer systems. Since the relative amount of heat conduction along the walls may greatly influence the heat transfer in entrance regions, these data are more specific than are the established region data.

REFERENCES

1. *Hamilton, D. C., Poppendiek, H. F., Redmond, R. F., and Palmer, L. D.: Free Convection in Fluids Having a Volume Heat Source (Theoretical Laminar Flow Analyses for Pipe and Parallel Plate Systems), ORNL-1769, Nov. 15, 1954.

2. Hamilton, D. C., Lynch, F. E., and Palmer, L. D.: The Nature of the Flow of Ordinary Fluids in a Thermal Convection Harp, ORNL-1624, Feb. 23, 1954.

3. Eckert, E.R.G., and Soehngen, E.: Interferometric Studies on the Stability and Transition to Turbulence of a Free Convection Boundary Layer, Proceedings of the General Discussion on Heat Transfer, 1951, p.321, Sponsored by IME and ASME.

*Reference 1 is a collection of three analyses originally distributed as
ORNL-CF 51-12-70, Dec., 1951,
ORNL-CF 52-1-1, Jan., 1952, and
ORNL-CF 52-1-2, Jan., 1952

APPENDIX A: APPARATUS AND PROCEDURE

It is recalled that the two-parallel-plate apparatus used for the velocity observations was identical in size and construction to the three-parallel-plate apparatus used for the heat transfer measurements with four exceptions; in the two-plate apparatus there were no wall temperature probe wells, d was equal to 0.75 inches, and, of course, there was no center plate. In addition, the fiber-frax insulation was only used on the sides of the two-plate apparatus thus leaving the line of sight unobscured in the y direction. Because of the semi-larity in the two systems the detailed description of the three-plate apparatus is considered to be adequate for both.

The semi-quantitative velocity measurements were made by observing the paths of small oil droplets* placed in the free convection stream and illuminated by a high intensity light source placed over the top of the system. This placed the source of the light at a right angle to the observer. The oil droplets were about 0.01 inches in diameter and had the same density as water when both were at about 83°F. Movable vertical cross hairs on the front and back faces permitted the observer to accurately sight along a line corresponding to the y direction and at a prescribed x position. Horizontal reference marks were scribed at vertical intervals of 0.5 inches. With this array of scribed lines and a stop watch the velocity of a droplet and its approximate position along the x axis could be measured. The value of X_i, the interface between the upward and downward moving streams, could be determined

---

*Merriam Company Unity Oil.

quite easily. The details of the construction of the two-plate apparatus are similar to those of the three-plate apparatus, the description of which follows immediately.

The Three-Parallel-Plate Apparatus

An overall view of the apparatus is shown in Figure 10 and a cross section is given in Figure 11. The system consists basically of the three plates or walls, the center wall and the right and left outer walls. The plastic bottom, top, front face and back face form the two identical free convection channels called the right and left test sections. A plate or wall parallel to and outside of each outer wall forms the coolant channel for removing the heat generated in the test section. The wall temperature measurements were made with thermocouple probes in the walls located in a plane parallel to the front and back faces and midway between them; i.e. the xz plane. The outer walls were constructed of 1/8 inch copper plate and the center wall was made of two 1/8 inch stainless steel plates put together with screws and then copper plated. Each test section was 0.5 in. x 6 in. x 36 in. and each guard heater section was about 0.5 in. x 0.75 in. x 36 in. The guard heater sections were formed by plastic spacers which inhibited fluid interchange between the guard heater sections and the test sections. The free convection test fluid was a dilute electrolyte. When the center wall was maintained at a given A.C. voltage while the two outer walls were electrically grounded the electrolyte acted as a resistance heater, each section being in parallel with the other. The center wall was constructed of stainless steel to give it stiffness and to reduce the heat conduction along the wall. It was copper plated so that the electrolyte would not be in contact with dissimilar metals and produce a galvanic cell

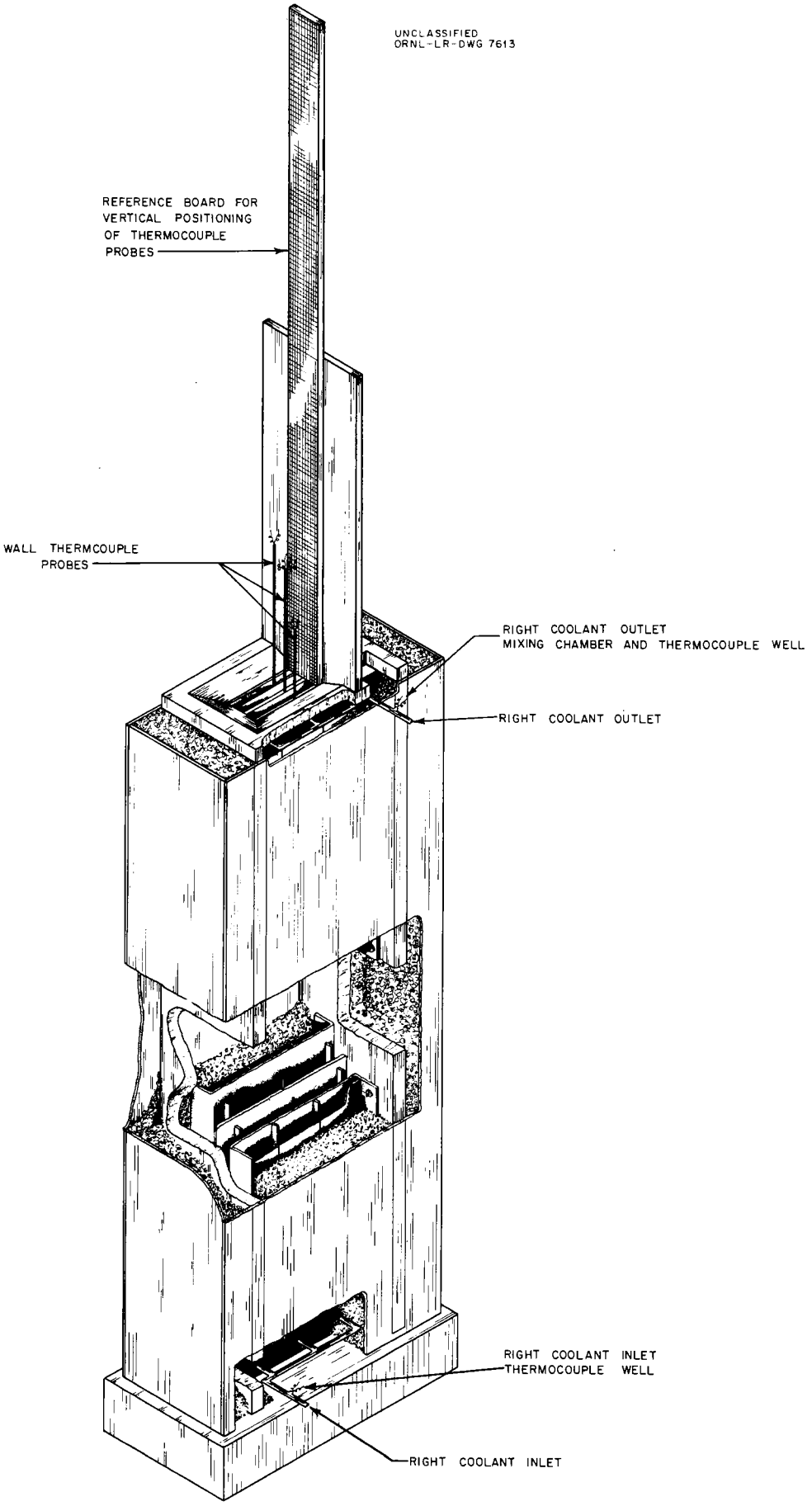

Fig. 10. Three-Parallel-Plate Apparatus

UNCLASSIFIED
ORNL-LR-DWG 7614

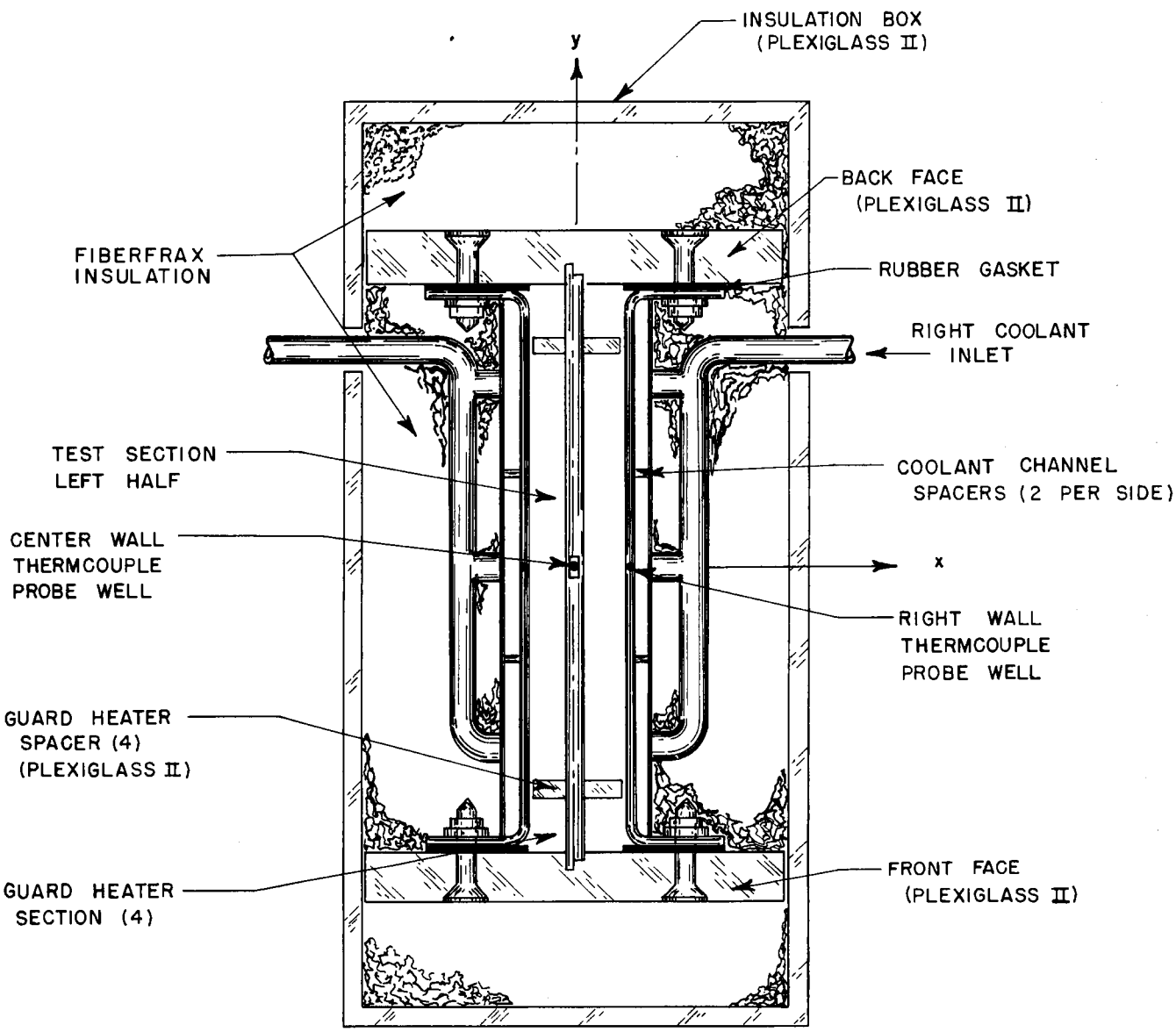

Fig. 11. Cross Section of Apparatus (Top View)

since all other metal components were made of copper. In the first design of the center wall it was made of plastic and covered with thin copper sheets. With this construction the guard heater sections and the test sections could be placed on separate electrical circuits. The plastic was not structurally capable of accurately maintaining the test section channel dimensions under operating temperatures so the stainless steel design was used. Thus, the principal function of the guard heater sections was to eliminate convection currents in the y direction in the test sections.

The flow area in each coolant channel was 3/16 in. x 8 in. Vertical spacers divided each coolant channel into three equal and parallel channels. In Figure 10 it is seen that the inlet and outlet coolant channel headers are reversed to provide the same pressure drop and therefore the same flow rate through each channel.

A plastic cover on the top of the test section prevented evaporation of the electrolyte. A reference board was attached to the top of the apparatus for positioning and holding the thermocouple wall probes.

It was important that the independent variables, power, coolant flow rate, and coolant inlet temperature, be constant with time and have the same value for each side of the system; i.e., the apparatus must be operated under conditions of steady state and symmetry about the yz plane. The power to the apparatus was supplied through a Sola constant voltage transformer, the power output of which was quite constant; having the two test sections wired in parallel tended to make the power distribution symmetrical. Measurements were made of the power, the current and the voltage. The average deviation of the apparent power factor, P/EI, from unity was calculated from these measurements to be $\pm$ 0.016. It is concluded that the actual power factor was probably near unity.

Each coolant channel circuit was independent of the other. The hot and cold water supply was provided with pressure regulators so that the coolant flow rate would be constant. With needle valves and calibrated rotometers each flow rate could be accurately set and measured. The hot water heater supplied water at a chosen temperature regulated to $\pm 2^{\circ}F$ or better. A water temperature regulator mixed the cold and hot water supplied to it to deliver any desired coolant water temperature with a variation of $\pm 1^{\circ}F$ or better.

The Determination of $x_o(y,z)$

Because the dimension, $x_o(y,z)$ was important, some care was taken in its determination. Special extension telescoping gages were used to survey the apparatus. A single survey consisted of 102 measurements in the test section and 68 measurements in the four guard heating sections.

Before the experimental program was started surveys were made for mean apparatus temperatures of 80, 95, 115, and 130°F. to determine the influence of temperature on $x_o(y,z)$; it was found that $x_o(y,z)$ increased at the rate of two percent per 100°F rise in temperature. This influence was accounted for in the evaluation of the data. For the remainder of this discussion it will be understood that the temperature is constant at 80°F.

A post-experimental program survey indicated that the value of $x_o(y,z)$ throughout the apparatus was rather uniformly less than the pre-experimental program value by about one percent. Accordingly, $x_o(y,z)$ values were used which were averages of the pre-experimental program survey and post-experimental program survey. From these average values the space average values $x_o(m,m)$ and $x_o(0,m)$ below were computed.

The space average value of $x_o(y,z)$ throughout the entire apparatus, $x_o(m,m)$, was 0.500 inches with maximum and minimum values of 0.518 inches and 0.481 inches, respectively; the average deviation in $x_o(m,m)$ was $\pm$ 0.007 inches. The mean value of $x_o(y,z)$ in the center-line region where all the wall temperatures were measured, $x_o(0,m)$, was 0.508 inches and the volume of the apparatus when filled to 35 inches was 264 cubic inches.

Instrumentation for Temperature Measurements

The temperature measurements were made using iron-constantan thermocouples. All thermocouples were calibrated by the authors at the steam point; in addition they were compared with N.B.S. calibrated precision mercury-in-glass thermometers in the intermediate range. The thermocouple voltage was measured with a Leeds and Northrup Special Thermal Free Wenner Type Potentiometer with an amplifier. The instrument could be read to 0.2 microvolt and the accuracy was at least as good as 1 microvolt or 0.03°F. In addition to measuring the temperature level above the ice point for each thermocouple the temperature difference between two thermocouples was measured directly when that was the reading desired.

Pyrex thermocouple wells were made for measuring the coolant inlet and outlet temperatures. A mixing chamber was placed directly upstream of the coolant outlet thermocouple wells to insure that the temperature measured actually was the mixed mean temperature.

The wall thermocouple probes are shown in Figure 12. The center wall probe position was fixed for the entire experiment. The three thermocouple junctions permitted temperatures to be measured at vertical positions corresponding to z_u = 21.1, z_m = 15, and z_ℓ = 10.5 inches. In order to save space in the pyrex tubing the three thermocouples used the same iron wire. The wires were No. 36 gage with a thin coating of Teflon for insulation. The outer wall probes used

UNCLASSIFIED
ORNL-LR-DWG 7615

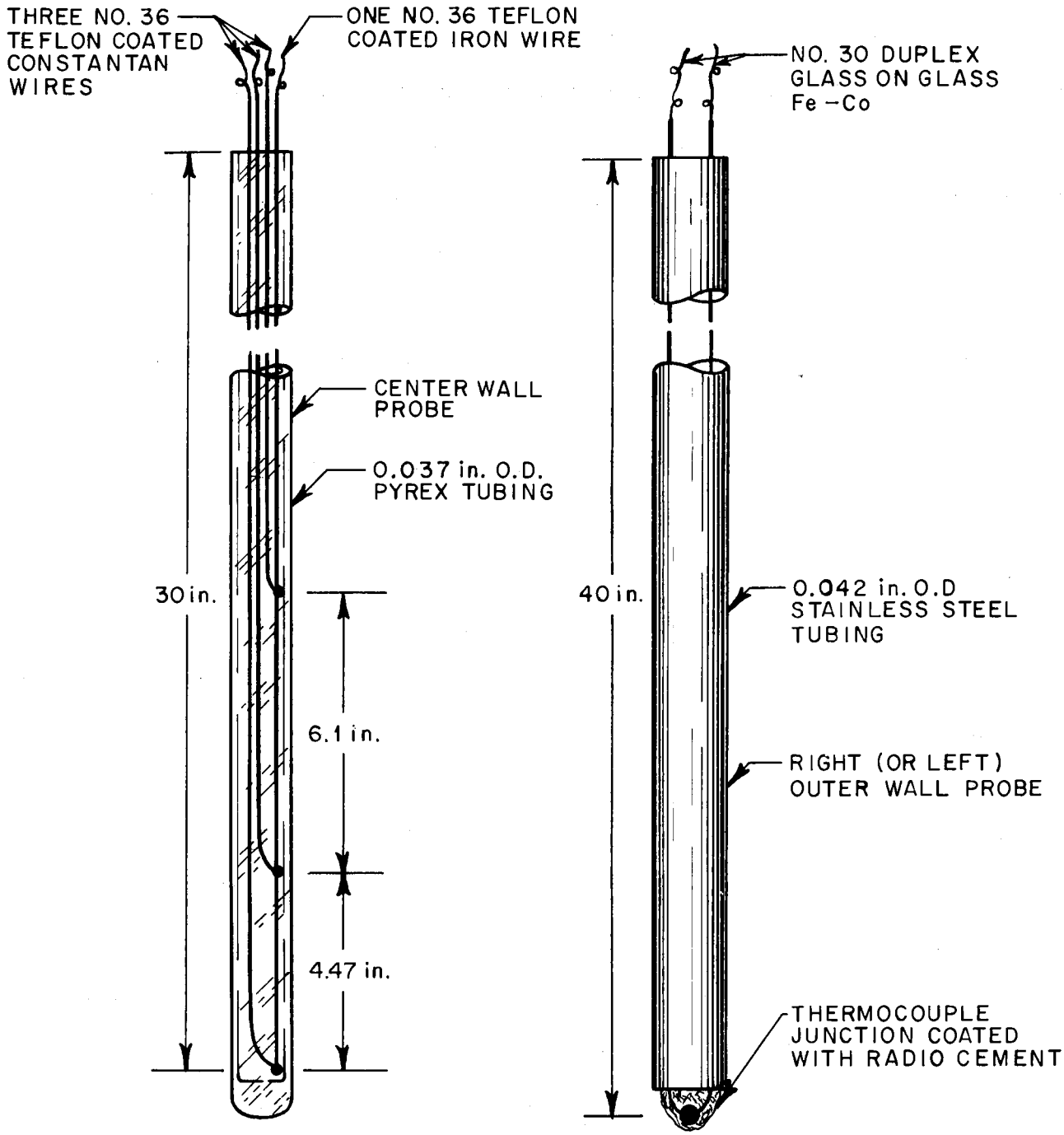

Fig. 12. Construction of Center and Outer Wall Thermocouple Probes

No. 30 gage Duplex glass-on-glass iron-constantan wires in a stainless steel capillary tubing. The thermocouple junction was coated with radio cement for electrical insulation.

In Figure 13 the thermocouple probe well construction is shown. The outer wall well was a 0.06 in. o.d. stainless steel tubing welded on the bottom end. A vertical slot, slightly deeper and wider than the tubing was milled in the back of the outer copper plate. The probe well tubing was inserted into the slot and the slot was filled with soft solder. The center-wall probe well was made of plastic. The original plans were to use a center wall probe identical to the outer wall probes. In the first test of the completed apparatus the hole in the center well became too small. In the subsequent attempt to enlarge the hole it could only be enlarged to z = 10.5 inches and it was damaged to the extent that it leaked. The only bad effect of the leak was to make the probe electrically charged. Due to lack of time the program was changed and the present three-thermocouple, stationary, pyrex, center-wall-probe was used.

After the last run the apparatus was disassembled and the left wall thermocouple probe well was found to be partly unsoldered over most of its length and completely unsoldered from z = 19 to z = 32 inches. The condition of the left well explained the consistently lower temperature data in the left wall; for that reason the left wall temperature data were not used. The right wall thermocouple well was found to be in perfect condition.

It was desired to settle the question of conduction error in the thermocouple probe design used. The right wall, with the coolant chamber removed, but with the thermocouple well left intact, had tubing attached at the top and bottom ends which acted as heat exchangers. When hot water was forced through the top exchanger and cold water through the bottom exchanger while the plate was

UNCLASSIFIED
ORNL-LR-DWG 7616

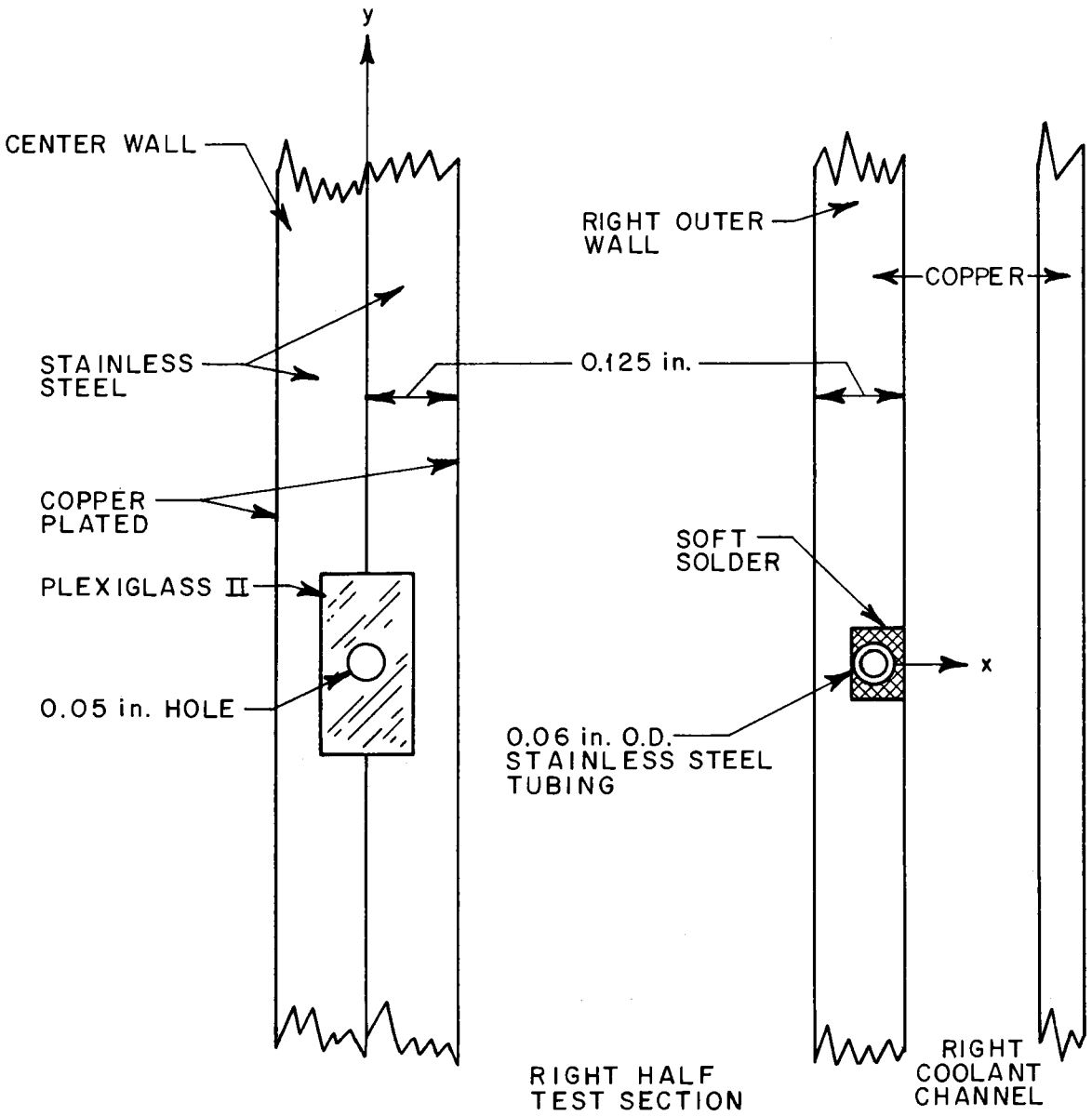

Fig. 13. Plan View Showing Center and Right Wall Thermocouple Probe Well Construction

surrounded with fiberfrax insulation it was easy to obtain a uniform vertical temperature gradient of 34 °F/ft. Calibrated thermocouples were spotted on the outside of the plate at various positions along the line of the well. With this arrangement the thermocouple probe could be calibrated under the actual conditions of use. The center wall and outer wall thermocouple probes were calibrated in the same way. The maximum difference in temperature between the probes and the reference thermocouples was 0.15 °F for an A of 34 °F/ft. The largest A used in the experiment was 28 °F/ft.

Procedure

A sample of the electrolyte was taken before and after each run and the electrical resistivity measured. The measurements that were recorded during the run were power, voltage, current, coolant flow rate, coolant inlet temperature and temperature rise, outer wall temperatures, the three center wall temperatures and the wall temperature differences. The wall temperatures were measured for 11 different vertical positions, three of which were, of course, at the levels of the center wall thermocouples. At each of the 11 positions all of the variables mentioned above were read and recorded. About 6 minutes were required for two observers to take the data per position, so 24 minutes were required to take the data at the positions z_u, z_{18}, z_m and z_ℓ. The maximum variation, which will hereafter be called the variation, in a given variable for these four readings is an indication of the constancy of that variable. To repeat, the variation of a variable for a run is defined as the difference in the maximum and minimum values of that variable, expressed in percent of the variable, recorded during the 24 minute interval discussed above. The average variation is the average of the absolute value of the variation for all the runs. The variation of the power was 2% maximum and 0.6% average. For the middle

center wall temperature, $t(0,z_m)$, the maximum and average variations were 0.3 ^oF and 0.08 ^oF, respectively: In percent of $\theta(0,z_m)$ these were 5% and 1.8%, respectively. One run was discarded due to a much greater variation in $t(0,z_m)$ which indicated that steady state had not been attained. For an individual coolant flow rate the maximum and average variations were 2.7% and 1.4%, respectively. The maximum and average variation for the individual coolant inlet temperatures were 0.3 ^oF and 0.13 ^oF, respectively: In percent of $\theta(0,z_m)$ these were 20% and 5%, respectively.

Another kind of variation of interest concerns the difference in a variable for the left and right side of the apparatus; this information gives an indication of the degree of asymmetry of the system. The maximum and average variations for the difference in the right and left coolant flow rates were 10% and 2.2%; in terms of the maximum coolant mixed mean temperature asymmetry this could produce at z_m, in percent of $\theta(0,z_m)$, these are 6% and 2.1%, respectively. Finally, the maximum and average variations for the difference in the right and left coolant inlet temperatures were 1^oF and 0.3 ^oF, respectively; in percent of $\theta(0,z_m)$ these are 14% and 8%, respectively.

There were three reservoirs exchanging heat in this experiment, the test section, the coolant, and the room air. The power, or the heat generated in the test section, Q_T, and the heat gained by the coolant, Q_C, were <u>measured</u> for each run. In order to make a heat balance it was necessary to be able to predict the exchange with the room air. In the following heat balance equations the double subscript indicates the heat transferred from the first reservoir to the second; e.g. Q_{TC} is heat transferred from the test section to the coolant and Q_{CR} is that transferred from the coolant to the room.

Thus:

$$Q_C = Q_{TC} - Q_{CR} \quad \ldots\ldots\ldots\ldots\ldots\ldots\ldots \quad (23)$$

$$Q_T = Q_{TC} + Q_{TR} \quad \ldots\ldots\ldots\ldots\ldots\ldots\ldots \quad (24)$$

subtracting, get

$$Q_T - Q_C = Q_{TR} + Q_{CR} \quad \ldots\ldots\ldots\ldots\ldots\ldots \quad (25)$$

With no liquid in the test section and coolant flowing through the apparatus the value of Q_{CR} was measured for several values of $(t_C - t_R)$. The resulting equation is:

$$Q_{CR} = 27(t_C - t_R) \quad \ldots\ldots\ldots\ldots\ldots\ldots \quad (26)$$

where Q_{CR} is in B/hr and t_C and t_R are in ^{o}F. The companion equation for Q_{TR} was determined from a numerical analysis to be:

$$Q_{TR} = 20(t_a - t_R) \quad \ldots\ldots\ldots\ldots\ldots\ldots \quad (27)$$

The heat balance for a run is defined in percent of Q_{TC} as:

$$H.B. = 100 \left[1 - \frac{Q_C + Q_{CR}}{Q_T - Q_{TR}} \right] \quad \ldots\ldots\ldots\ldots \quad (28)$$

The average value of the heat balance for all the runs was $\pm$ 9.4% and the extreme values were -15% and +33%.

APPENDIX B: TREATMENT OF THE DATA

The electrolyte resistivity was not independent of temperature so the power distribution was not entirely uniform as was postulated in the theoretical analysis. In order to make a meaningful comparison of theory and experiment it was necessary to analyze the data to account for this non-uniform power distribution - or show that the influence is negligible. To accomplish this purpose it was first necessary to determine the properties of the electrolyte; the discussion of this determination is given in the next section. Following that the proposed method for determining the conduction temperature difference at a given position in such a system is derived in two steps. Finally, a brief description is given of the data analysis.

Properties of the Electrolyte

The very dilute HCl in distilled water solution used as the electrolyte was assumed to have the physical properties of liquid water. The properties k, N_{Pr}, and $\left(\frac{\beta_V}{\alpha\nu}\right)$ that were used in analyzing the data are plotted in Figure 14 and are based on the handbook values of the physical properties of water.

Electrical properties of the electrolyte were measured by the authors using a calibrated "Industrial Instruments Model RC 16" 1000 cycle per second conductivity bridge and a conductivity cell having a cell constant of unity. The bridge was calibrated with standard resistors and the conductivity cell constant was determined using a standard KCl solution. The cell electrodes were frequently and carefully platinum-blacked. The solution sample was placed in a constant temperature bath during the measurements and the temperature was measured with a NBS calibrated mercury-in-glass thermometer with smallest intervals of $0.2^{o}F$.

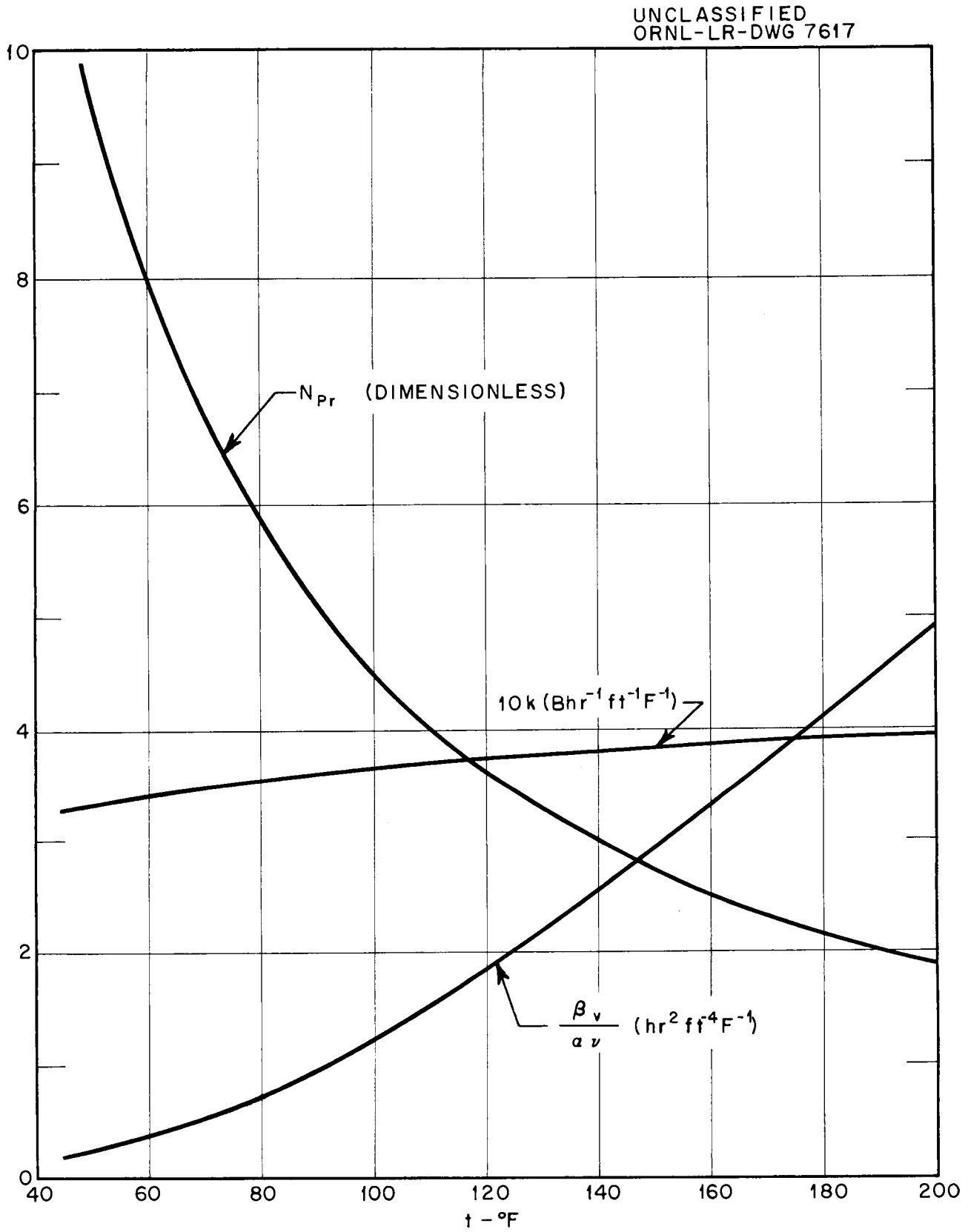

Fig. 14. Selected Physical Properties of Liquid Water

The resistivity of the solution was measured before and after each run. For the 28 runs the most concentrated and the most dilute solutions used had resistivity values at 80°F of 25,000 and 38,000 ohm-cm, respectively. The resistivity versus temperature curves for two solutions are shown in Figure 15. The values of β_r and β_{rk} in Figure 16 were computed from the data shown in Figures 14 and 15.

Derivation of the Method for Computing $\theta^*_c(0,z)$

It is desired to compute $\theta_c^*(0,z)$ from total power measurements and the known variation of $x_o(y,z)$ and $r(t)$ in the experimental apparatus. A concerted effort was made in the design of the apparatus to minimize the variation of temperature in the y direction. This effort was certainly successful to the extent that this variation may be neglected in the present analysis. As a result of this assumption the resistivity is a function of only X and z: That is, $r(X,z)$. The variation of $x_o(y,z)$ with y will be considered.

The electrical circuit for the apparatus caused the center wall to be charged and the right and left walls to be at ground potential. This caused each elemental volume of electrolyte $x_o(y,z)dydz$ to have the same impressed voltage and to be in parallel with all other elements, thus minimizing the influence of the variation of $x_o(y,z)$ on $\theta_c^*(y,z)$.

The power generated in the volume $x_o(y,z)dydz$ is:

$$d^2P(y,z) = \frac{E^2}{r(m,z)\ x_o(y,z)}\ dydz \quad \ldots\ldots\ldots\ldots\ldots \quad (29)$$

where $r(m,z) = \int_0^1 r(X,z)dX.$

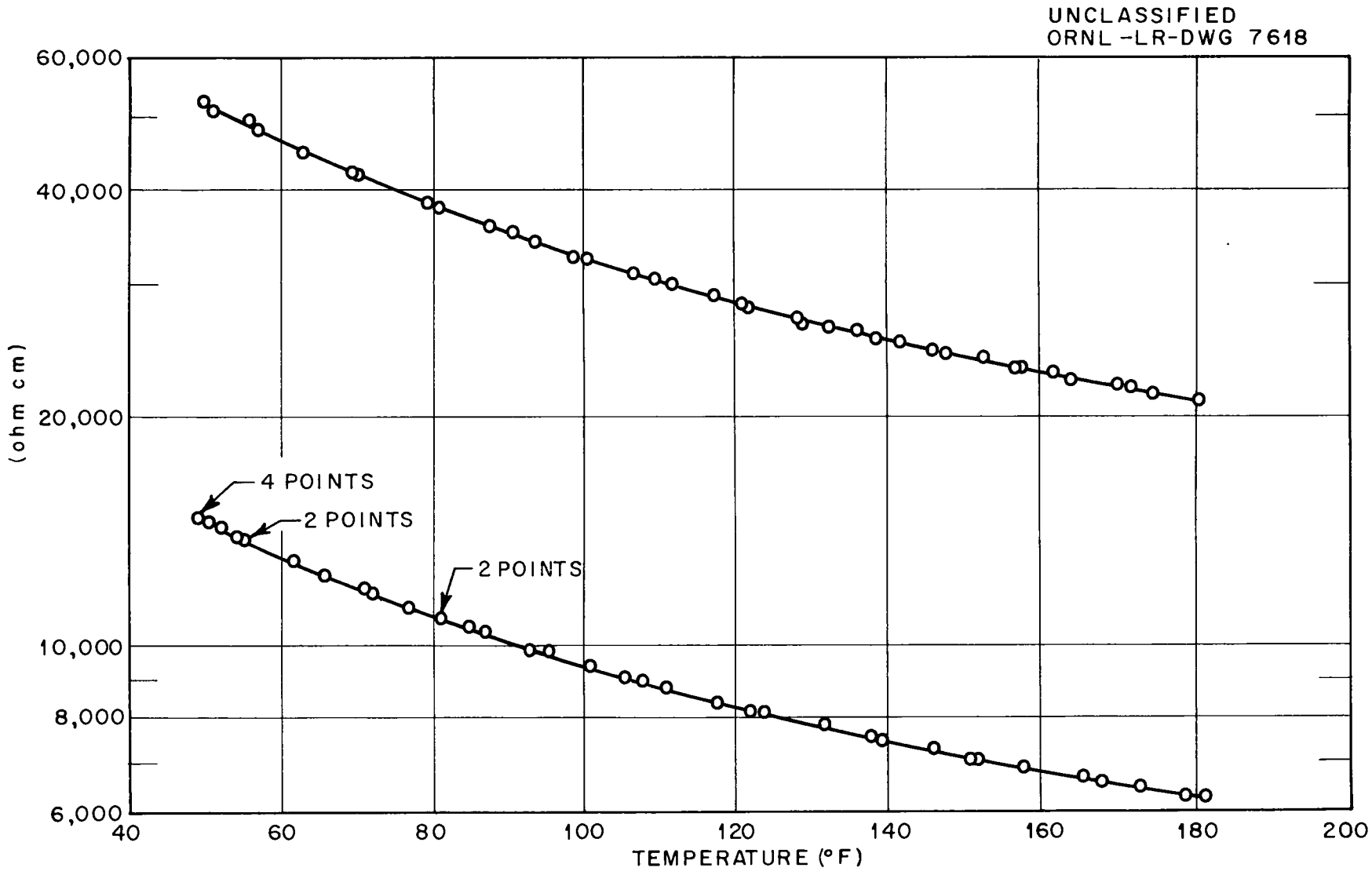

Fig. 15. Electrical Resistivity of Two HCl in H_2O Solution

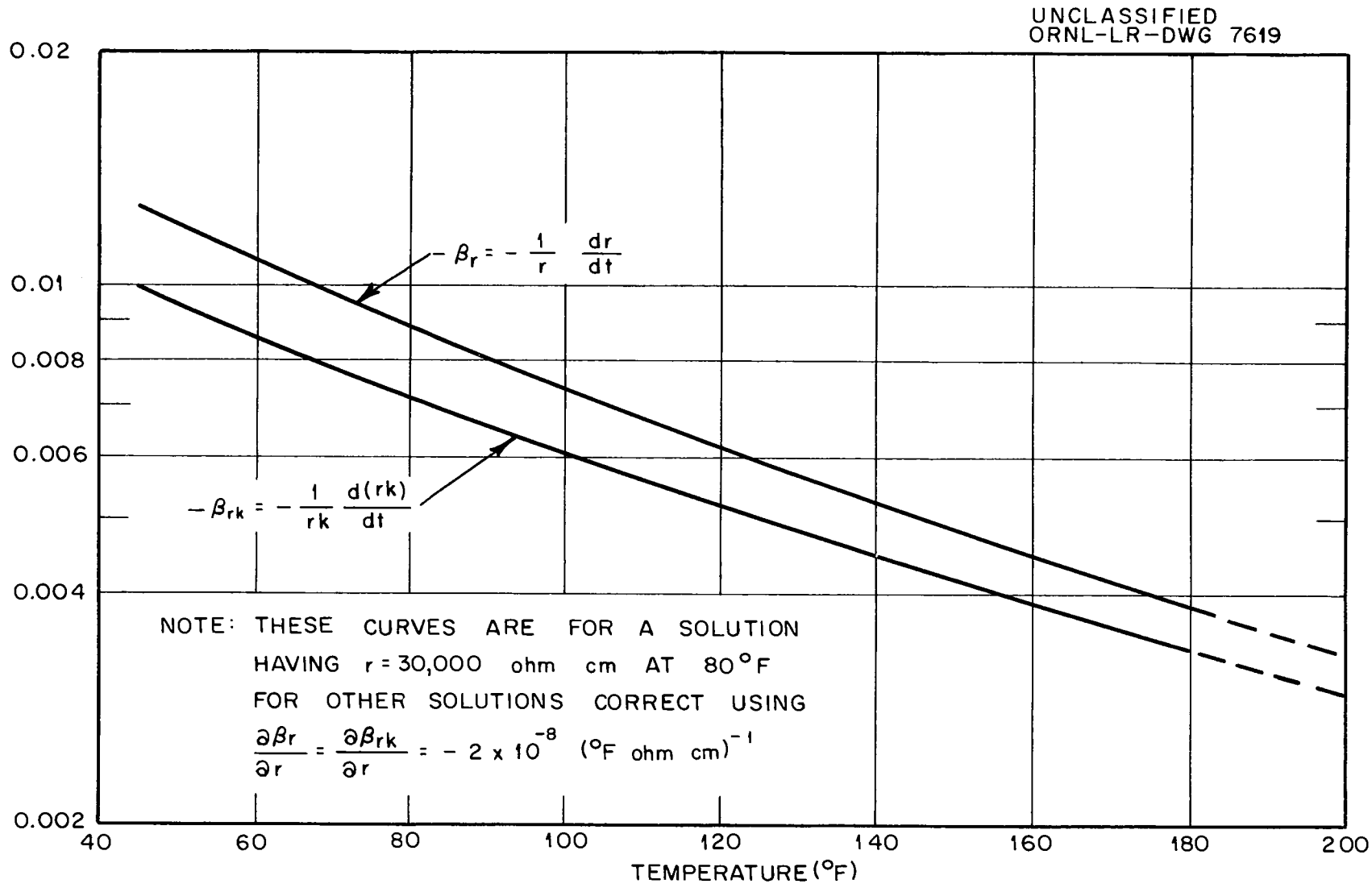

Fig. 16. Electrolyte Temperature Coefficients β_r AND β_{rk}

The mean volume heat source term is:

$$q'''(m,y,z) = \frac{d^2P(y,z)}{x_o(y,z)dydz} = \frac{E^2}{r(m,z)\ x_o^2(y,z)} \quad \cdots\cdots\cdots\cdots \quad (30)$$

Thus,

$$\theta_c^*(0,y,z) = \frac{q'''(m,y,z)\ x_o^2(y,z)}{2k} = \frac{E^2}{2kr(m,z)} \quad \cdots\cdots\cdots \quad (31)$$

From Equations (29), (30) and (31) it is seen that the power, $d^2P(y,z)$, and the source term, $q'''(m,y,z)$, depend on $x_o(y,z)$ but $\theta_c^*(0,y,z)$ does not.

One obvious method of computing $\theta_c^*(0,y,z)$ is from Equation (31) using r and E measurements. The method preferred by the authors is based on measurement of volume and total power. For the following discussion let a volume heat source be defined in terms of the measured total power, P, and total volume, v, as follows:

$$q_o''' = \frac{P}{v} \quad \cdots\cdots\cdots\cdots\cdots\cdots\cdots\cdots\cdots \quad (32)$$

Integration of Equation (29) gives:

$$P = E^2 \int_{-y_o}^{+y_o} \int_{0}^{z_o} \frac{dydz}{x_o(y,z)\ r(m,z)} \quad \cdots\cdots\cdots\cdots \quad (33)$$

Since the total variation in $x_o(y,z)$ is less than 8 percent and that of $r(m,z)$ less than 20 percent for these experiments, the influence of each on the power distribution may be considered independently without great error. That is to say:

$$\int_{-y_o}^{y_o} \int_{0}^{z_o} \frac{dydz}{x_o(y,z)\ r(m,z)} \cong \left\{ \int_{-y_o}^{y_o} \int_{0}^{z_o} \frac{dydz}{x_o(y,z)} \right\} \left\{ \int_{-y_o}^{y_o} \int_{0}^{z_o} \frac{dydz}{r(m,z)} \right\}$$

Let us first determine the influence of $x_o(y,z)$ by considering $r(m,z)$, and k to be constant and equal to $\overline{rk}$. Thus:

$$\theta_c^*(0,y,z) = \frac{E^2}{2\overline{rk}} = \text{constant} \quad \ldots\ldots\ldots\ldots \tag{31a}$$

and

$$P = \frac{E^2}{\overline{r}} \int_{-y_o}^{y_o} \int_{0}^{z_o} \frac{dydz}{x_o(y,z)} \quad \ldots\ldots\ldots\ldots\ldots \tag{33a}$$

But, since the variation of $x_o(y,z)$ is small

$$\int_{-y_o}^{y_o} \int_{0}^{z_o} \frac{dydz}{x_o(y,z)} \cong y_o^2 \, z_o^2 \left[\int_{-y_o}^{y_o} \int_{0}^{z_o} x_o(y,z)dydz \right]^{-1} = \frac{v}{x_o^2(m,m)}$$

and

$$P = \frac{E^2 v}{\overline{r}\, x_o^2(m,m)} \quad \ldots\ldots\ldots\ldots\ldots\ldots\ldots\ldots \tag{33b}$$

From Equations (31a), (32), (33b), get:

$$\theta_c^*(0,y,z) = \frac{q'''_o \, x_o^2(m,m)}{2k} \quad \ldots\ldots\ldots\ldots\ldots \tag{34}$$

Now, to determine the influence of $r(m,z)$, Equation (29) is integrated considering $x_o(y,z)$ to be uniform and equal to $x_o(m,m)$.

Since $\beta_r \left[t_m(z) - t_m(z_a) \right]$ is small, one can write:

$$\frac{1}{r(m,z)} \cong \frac{1}{r(m,z_a)} \left[1 - \beta_r \left(t_m(z) - t_m(z_a) \right) \right] \quad \ldots\ldots\ldots \tag{35}$$

Putting Equation (35) in Equation (29) and integrating, get:

$$P = \frac{E^2 \, v \, K(z_a)}{x_o^2(m,m) \; r(m,z_a)} \quad \ldots\ldots\ldots\ldots\ldots\ldots\ldots \tag{36}$$

where
$$K(z_a) = 1 - \frac{\beta_r}{z_o} \int_0^{z_o} \left[t_m(z) - t_m(z_a)\right] dz \quad \ldots\ldots\ldots \quad (37)$$

$$q'''(z_a) = \frac{q'''_o}{K(z_a)} \quad \ldots\ldots\ldots\ldots\ldots\ldots\ldots \quad (38)$$

$$\theta_c{*}(0,z_a) = \frac{q'''_o \; x_o^2(m,m)}{2k(z_a) \; K(z_a)} \quad \ldots\ldots\ldots\ldots\ldots \quad (39)$$

The distribution in power due to the variation in x_o while r was held constant resulted in the $\theta_c{*}(0,y,z)$ given by Equation (34); the value of $\theta_c{*}(0,z_a)$ for a system in which x_o was held constant and the variation in r was considered is given in Equation (39). When the two results are combined to account for the nonuniformity of both x_o and r the following are the results for the location y = 0 and z = z_a:

$$q'''(m,z_a) = \frac{q_o'''}{K(z_a)} \; \frac{x_o^2(m,m)}{x_o^2(0,z_a)} \quad \ldots\ldots\ldots\ldots\ldots \quad (40)$$

Now, by definition:

$$\theta_c{*}(0,z_a) \equiv \frac{q'''(m,z_a) \; x_o^2(0,z_a)}{2k(z_a)} \quad \ldots\ldots\ldots\ldots \quad (41)$$

Thus:
$$\theta_c{*}(0,z_a) = \frac{q'''_o \; x_o^2(m,m)}{2k(z_a) \; K(z_a)} \quad \ldots\ldots\ldots\ldots\ldots\ldots \quad (42)$$

The values of $K(z_a)$ were computed from Equation (37) and the temperature data for Runs 17 and 20 as 1.001 and 1.003, respectively. It was concluded that $K(z_a)$ could be assumed to be unity for these experiments.

From Equation (31) obtain

$$\frac{\theta_c{*}(0,z)}{\theta_c{*}(0,z_a)} = \frac{k(z_a) \; r(z_a)}{k(z) \; r(z)} = 1 - \beta_{rk} \left(t_m(z) - t_m(z_a)\right) \quad \ldots\ldots \quad (43)$$

From Equations (42) and (43) the value of $\theta_c^*(0,z)$ may be computed from the total power, total volume and the physical properties of the electrolyte.

Derivation of the Method for Computing $\theta_c(0,z)$

In the experimental system the electrolyte resistivity, r, was temperature sensitive and, therefore the volume heat source, q''', was a function of temperature. There follows a computation of $\theta_c(0)$ and t_m for a conduction system in which the source term, q''', varies in accordance with a temperature distribution similar to that in the free convection system analyzed in this report. Since z is constant during this analysis the function $\theta_c(X,z)$ is written as $\theta_c(X)$ for brevity.

The equation to be solved is:

$$\frac{d^2\theta_c(x)}{dx^2} = -\frac{q'''(x)}{k} \quad \ldots\ldots\ldots\ldots\ldots\ldots \quad (44)$$

The postulates that define the system are:

1. k is uniform (in the experiment it is evaluated at t_a)
2. $q'''(X) = q'''(m)\left[1 + \beta_r\,\theta_c^*(0)\left(\Phi^*(X) - \Phi^*(m)\right)\right]$

   where $q'''(m) = \int_0^1 q'''(X)\,dX = q'''(t_m)$
3. The free convection temperature distribution can be satisfactorily approximated by:

$$\Phi^*(X) = \Phi^*(0) \qquad \text{for} \quad 0 \leq X \leq X_c$$

$$\Phi^*(X) = 1-X^2 \qquad \text{for} \quad X_c \leq X \leq 1$$

where $X_c = \sqrt{1 - \Phi^*(0)}$

From (3) above one can compute the mean temperature for evaluating q''' as

$$\Phi^*(m) = \int_0^{X_c} \Phi^*(0)\, dX + \int_{X_c}^{1} (1-X^2)\, dX$$

$$\Phi^*(m) = \frac{2}{3}\left(1 - X_c^3\right)$$

or

$$1 - \frac{\theta(m)}{\theta(0)} = 1 - \frac{2}{3}\left\{\frac{1 - \left(1 - \Phi^*(0)\right)^{3/2}}{\Phi^*(0)}\right\} \equiv F_1 \ldots \qquad (45)$$

Now, Equation (44) may be written:

$$\frac{d^2\Phi^*_c(X)}{dX^2} = -2\left\{1 + \beta_r\theta^*_c(0)\left(\Phi^*(X) - \Phi^*(m)\right)\right\} \ldots \qquad (44a)$$

with boundary conditions $\frac{d\Phi^*_c(0)}{dX} = 0$ and $\Phi^*_c(1) = 0$.

The desired solution is:

$$\Phi^*_c(0) = 1 + \beta_r\, \theta^*_c(0)\, F_2 \ldots\ldots\ldots\ldots \qquad (46)$$

Where

$$F_2 \equiv \frac{1}{6}\left\{4 - 6\Phi^*(0) + 3\left[\Phi^*(0)\right]^2 - 4\left[1 - \Phi^*(0)\right]^{3/2}\right\}\ldots\ldots \qquad (47)$$

or

$$\theta_c(0) = \theta_c^*(0)\left\{1 + \beta_r\, \theta^*_c(0)\, F_2\right\}\ldots\ldots\ldots\ldots\ldots \qquad (48)$$

The mean temperature, t_m, is computed from Equation (45) as

$$t_m = t(0) - \theta(0)\, F_1 \ldots\ldots\ldots\ldots\ldots\ldots\ldots \qquad (49)$$

F_1 and F_2 are plotted in Figure 17.

The Data Analysis

Reference to Figures 5 and 6 in the RESULTS AND DISCUSSION section may aid in the understanding of the data analysis. From the power, the volume, and

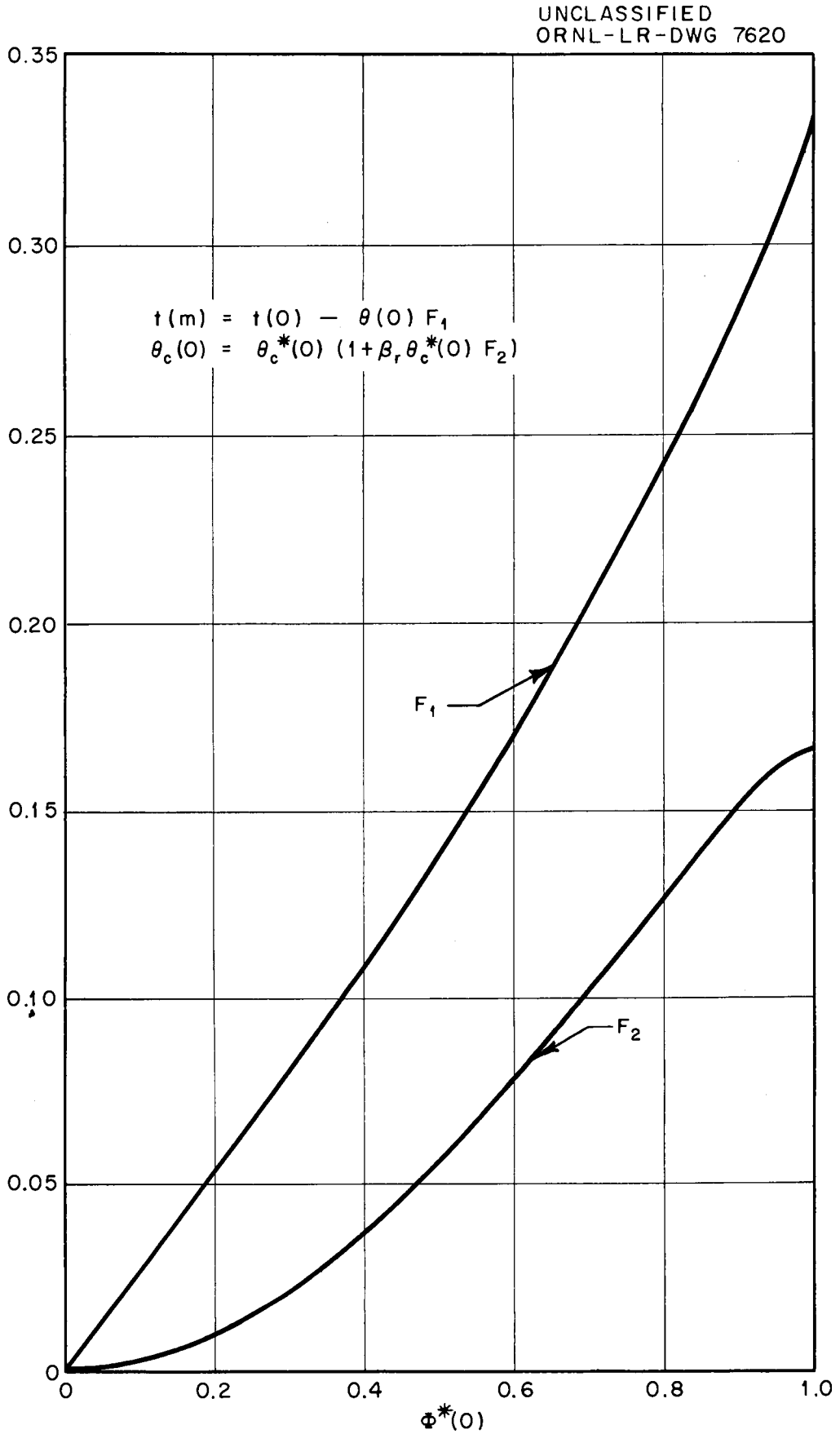

Fig. 17. The Factors F_1 and F_2 for Computing $t(m)$ and $\theta_c(0)$

the temperature data such as is shown on Figure 5 it is desired to determine N_I, N_{II}, N_{III}, $\left[\Phi(0,z)\right]_{min}$ and $\Phi(0,z_o)$. The temperature gradient in the outer wall, A(1), was obtained graphically from the mean line drawn through the right wall temperature data. The gradient in the center wall was computed from the measured temperature difference $\left[t(0,z_m) - t(0,z_\ell)\right]$ and the known value of $(z_m - z_\ell)$. The average temperature of the fluid, t_a, at the average height, z_a, was used to evaluate the properties $(\beta_v/\alpha\nu)$, N_{Pr}, k, in computing N_I, N_{II}, and N_{III}; the value of x_o and the volume was also compensated for temperature change by using t_a as the representative apparatus temperature. It is recalled that, for $t_a = 80^oF$, $x_o(m,m) = 0.500$ inches, $x_o(0,m) = 0.508$ inches, and for $z_o = 35$ inches the volume was equal to 264 cubic inches. Also, the temperature influence on x_o and v were:

$$\frac{1}{x_o}\frac{dx_o}{dt_a} = \frac{1}{v}\frac{dv}{dt_a} = 2 \times 10^{-4}\ {}^oF^{-1} \quad \ldots\ldots\ldots\ldots\ldots \qquad (50)$$

The significant dimension used in computing <u>all</u> factors was $x_o(0,m)$ which was the average value in the region where the temperature measurements were made. Recall that $\theta_c{*}(0)$ is the conduction temperature difference in a system in which the volume heat source term is <u>uniform</u>.

The quantity $\theta{*}_c(0,z_a)$ was computed for z_a using Equation (42), with $K(z_a) = 1$, and is the value of $\theta{*}_c(0)$ that would exist in a system having a uniform volume heat source term equal to $q'''(m,z_a)$, the mean source term that did exist at z_a in the experimental system. With Equation (43) the value of $\theta{*}_c(0,z)$ could be computed for any z in terms of $\theta{*}_c(0,z_a)$.

The influence on $\theta_c(0)$ of the variation of the volume heat source term with X was given in Equation (48) in terms of $\theta_c{*}(0)$. The value of $\Phi(0,z_u)$, $\Phi(0,z_m)$ and $\Phi(0,z_\ell)$ were computed from the $\theta(0)$ data, Equations (42), (43), (48), and (49), and Figure 17. In Figure 6 the graphical determination of $\theta(0,z_o)$ and $\left[\Phi(0,z)\right]_{min.}$ is shown for the five different types of data that were obtained.

The average difference in the value of $\theta_c(0)$ and $\theta_c{*}(0)$ for all the runs was 0.25 percent and the maximum difference was less than one percent. This is further evidence that the source term could be assumed to be uniform in the X direction for the present experiments.